

Towards Federated Graph Learning in One-shot Communication

Guochen Yan Xunkai Li Luyuan Xie Wentao zhang Qingni Shen Yuejian Fang Zhonghai Wu

Abstract

Federated Graph Learning (FGL) has emerged as a promising paradigm for breaking data silos among distributed private graphs. In practical scenarios involving heterogeneous distributed graph data, personalized Federated Graph Learning (pFGL) aims to enhance model utility by training personalized models tailored to client needs. However, existing pFGL methods often require numerous communication rounds under heterogeneous graphs, leading to significant communication overhead and security concerns. While One-shot Federated Learning (OFL) enables collaboration in a single round, existing OFL methods are designed for image-centric tasks and ineffective for graph data, leaving a critical gap in the field. Additionally, personalized models derived from existing methods suffer from bias, failing to effectively generalize to the minority. To address these challenges, we propose the first **One-shot personalized Federated Graph Learning** method (**O-pFGL**) for node classification, compatible with Secure Aggregation protocols for privacy preservation. Specifically, for effective graph learning in one communication round, our method estimates and aggregates class-wise feature distribution statistics to construct a global pseudo-graph on the server, facilitating the training of a global graph model. To mitigate bias, we introduce a two-stage personalized training approach that adaptively balances local personal information and global insights from the pseudo-graph, improving both personalization and generalization. Extensive experiments on 12 multi-scale graph datasets demonstrate that our method significantly outperforms state-of-the-art baselines across various settings.

1. Introduction

Graphs are widely employed to model complex relationships between entities across a variety of domains (He et al., 2023; Hyun et al., 2023; Bang et al., 2023). While various algorithms and models (Gasteiger et al., 2018; Iscen

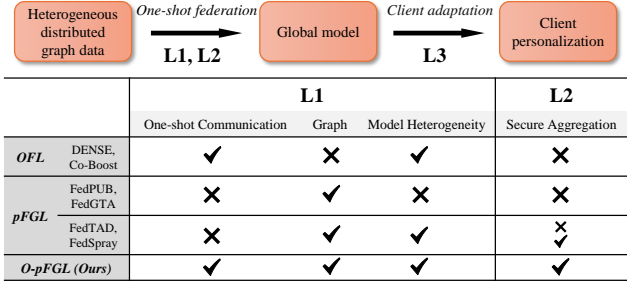


Figure 1: The key limitations of existing methods. Our method stands out as the only method capable of supporting one-shot federated learning for graph data while accommodating model heterogeneity and Secure Aggregation.

et al., 2019; Wu et al., 2020) have been proposed, most of them assume that graph data from different sources are managed centrally. However, collecting and managing such graph data is often costly, impractical, and poses significant privacy risks in many sensitive scenarios (Fu et al., 2022).

To address the tension between the need for vast datasets and the growing demand for privacy protection, Federated Graph Learning (FGL) has emerged as a promising solution, which enables collaborative training on distributed graph data without requiring centralized management (Pan et al., 2023; Gu et al., 2023). While FGL shows its potential, it faces two major limitations: (1) Typical FGL struggles to effectively personalize models for joint improvement across heterogeneous clients' graph data. This heterogeneity arises from variations of both node and structural properties, with adjacent nodes influencing each other, further complicating personalization. (2) FGL requires iterative communication between clients and the server, raising efficiency concerns due to communication overhead (Kairouz et al., 2021; Dai et al., 2022) and security concerns (e.g. man-in-the-middle attacks (Wang et al., 2020; Mothukuri et al., 2021; Zhu et al., 2024a)). These limitations can be mitigated by integrating personalized federated graph learning (pFGL) and one-shot federated learning (OFL), which offer novel solutions to improve communication efficiency and model personalization.

To address these challenges, we explore the integration of pFGL and OFL. The pFGL methods allow for per-

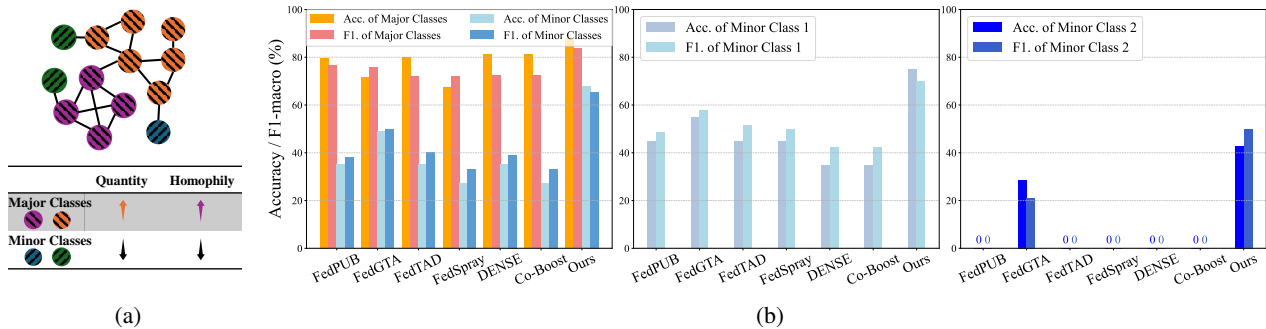


Figure 2: **(a) A toy example** explains the major classes and minor classes. **(b) The empirical analysis** of a client on the CiteSeer dataset under the Louvain partition to illustrate **L3**. Left: Existing methods result in a biased model that neglects the minority. Middle: The performance of existing and our methods in class 1 with 50 samples. Right: The performance of existing and our methods in class 2 with 14 samples. Our method effectively mitigates the performance gap.

sonalized model training by focusing on individual client graph data. OFL methods limit communication to a single round, thereby reducing the communication overhead and circumventing security risks such as man-in-the-middle attacks (Guha et al., 2019; Zhang et al., 2022). However, both existing pFGL and OFL methods face challenges in FGL. Specifically, they exhibit the following limitations:

L1: Ineffectiveness for graph learning in one communication round. Existing pFGL methods (Baek et al., 2023; Li et al., 2024b; Zhu et al., 2024b) rely on iterative communication for optimization, making them ineffective within one communication round. Most methods also fail to support heterogeneous models, as they primarily rely on aggregating model parameters. Meanwhile, existing OFL methods, which focus primarily on image-centric tasks, are incompatible with graph data. The ensemble-based OFL methods (Zhang et al., 2022; Dai et al., 2024) can invert images from ensemble models, but struggle with graph data due to the inter-dependencies between nodes. The distillation-based OFL faces the problems of distilling inter-related graphs. The generative-based OFL methods (Heinbaugh et al., 2023; Yang et al., 2024b;a) rely on pre-trained generative models (e.g. Stable Diffusion (Rombach et al., 2022)), which are not suitable for graph generation.

L2: Incompatibility with Secure Aggregation. Secure Aggregation is a widely used protocol (Bonawitz et al., 2017; So et al., 2022) designed to safeguard client privacy during the federated aggregation process. However, most pFGL and OFL methods require clients to upload raw model parameters or auxiliary information independently, which complicates the aggregation process (e.g. ensemble or similarity calculation) and hinders the implementation of privacy-preserving weighted averages.

L3: Imbalance between personalization and local generalization in personalization. Local graph data often exhibit

a significant imbalance in both quantity and topology, as illustrated in Figure 2a. Personalized models tend to be biased toward major classes (with larger quantities and high homophily to form compact communities), while neglecting minor classes with fewer samples and often surrounded by nodes from major classes. This imbalance leads to a degradation in overall model performance, particularly in underrepresented classes. A detailed empirical analysis is provided in Figure 2b, which shows that existing personalized methods result in heavy bias toward majority classes (class 3 and class 5, with a total of 180 samples) while failing to adequately represent minority classes (class 1 and class 2, with only 64 samples), highlighting the limitations of current methods in handling imbalanced graph data.

To overcome these limitations, we propose a **One-shot personalized Federated Graph Learning method (O-pFGL)**. Our method supports model heterogeneity and Secure Aggregation protocols for privacy preservation. Specifically, for **L1** and **L2**, clients upload estimated feature distribution statistics, augmented by our proposed homophily-guided reliable node expansion strategy, instead of raw model parameters. The server securely aggregates these statistics to generate a global pseudo-graph, which is subsequently utilized to train personalized models on clients, eliminating the need for direct model parameter exchanges and preventing model theft. To address **L3**, we propose a two-stage personalized training approach. In the first stage, clients train a global model based on the pseudo-graph, which serves as both a fixed teacher capturing global knowledge and a start-point for subsequent fine-tuning. In the second stage, clients fine-tune the global model on local graph data with the node-adaptive distillation, which leverages the global knowledge from the teacher model to counteract biases toward majority, ensuring effective learning for minority and achieving a robust balance between personalization and generalization.

Our method significantly outperforms state-of-the-art baselines through comprehensive experiments across various settings, including different graph scales, partition strategies, learning paradigms, and evaluation metrics. Experimental results demonstrate the superiority of our method in achieving a one-shot personalized federated graph learning solution that balances efficiency, privacy, and personalization. To sum up, our contributions are listed as follows:

- **Bridge the Gap.** To the best of our knowledge, we are the first to investigate the one-shot personalized federated graph learning problem under both graph data heterogeneity and model heterogeneity.
- **Novel Solution.** We propose a novel method that aggregates client statistics rather than model parameters to generate a global pseudo-graph, which is used for two-stage personalized training with node-adaptive distillation. Our method is compatible with Secure Aggregation and protects models’ intellectual property.
- **SOTA Performance.** We conduct extensive experiments on 12 multi-scale graph datasets across various settings and demonstrate the superiority of our method.

2. Related Works

2.1. Federated Graph Learning

From the graph level (Xie et al., 2021; Tan et al., 2023), each client possesses multiple independent graphs (e.g. molecular graphs) and target graph-level downstream tasks. From the subgraph level, each client possesses a subgraph of an implicit global graph. FedPUB (Baek et al., 2023) and FedGTA (Li et al., 2024b) personalizes model by similarity of functional embedding and mixed moments of neighbor features. AdaFGL (Li et al., 2024a) studies the structure non-IID problem. FedTAD (Zhu et al., 2024b) performs data-free distillation on the server. To complete missing connections between subgraphs, FedSage (Zhang et al., 2021) and FedDEP (Zhang et al., 2024) additionally train a neighborhood generator. To better represent the minority in local graph data, FedSpray (Fu et al., 2024) learns class-wise structure proxies to mitigate biased neighborhoods. But it needs numerous communication rounds for optimization.

2.2. One-shot Federated Learning

One-shot federated learning largely reduces communication costs and circumvents potential man-in-the-middle attacks. Mainstream OFL methods can be classified into 3 categories. (1) Ensemble-based methods (Guha et al., 2019; Zhang et al., 2022; Dai et al., 2024), (2) Distillation-based methods (Zhou et al., 2020; Song et al., 2023), (3) Generative-based methods (Heinbaugh et al., 2023; Yang et al., 2024a;b). However,

existing OFL methods primarily focus on image data and are either incompatible or ineffective for graph learning.

3. Preliminaries

3.1. Notations and Definitions

Consider a federated graph learning setting with m clients, where k -th client possesses the local undirected graph $G_k(\mathcal{V}_k, \mathcal{E}_k)$ with $|\mathcal{E}_k|$ edges and $|\mathcal{V}_k| = N_k$ nodes. Node features matrix is $\mathbf{X}_k = \{\mathbf{x}_1, \dots, \mathbf{x}_{n_k}\} \in \mathbb{R}^{|\mathcal{V}_k| \times f}$, where f denotes the feature dimension and \mathbf{x}_i is the feature of node v_i . The adjacency matrix is \mathbf{A}_k and augmented normalized adjacency matrix is $\tilde{\mathbf{A}}_k$. The labels of nodes in this local graph are denoted by $\mathbf{Y}_k = \{y_1, \dots, y_{n_k}\} \in \mathbb{R}^{|\mathcal{V}_k| \times C}$, where C denotes the number of distinct classes. In the semi-supervised node classification task (Kipf & Welling, 2016), nodes on k -th client are partitioned into labeled nodes $\mathcal{V}_{k,L}$ and unlabeled nodes $\mathcal{V}_{k,U}$. The corresponding labels are $\mathbf{Y}_{k,L}$ and $\mathbf{Y}_{k,U}$, respectively. The neighborhood of node v_i in $G_k(\mathcal{V}_k, \mathcal{E}_k)$ is defined as $\mathcal{N}_{v_i} = \{u | \exists e_{u,v_i} \in \mathcal{E}_k\}$, where edge e_{u,v_i} connects node u and v_i .

Definition 3.1. Node Degree. For node v_i in an undirected graph $G(\mathcal{V}, \mathcal{E})$, the node degree $d(v_i)$ is the number of edges connected to v_i . Formally, $d(v_i) = |\{e_{v_i,u} | u \in \mathcal{V}\}|$.

Definition 3.2. Node Homophily. For a labeled node $v_i \in \mathcal{V}_L$ in an undirected graph $G(\mathcal{V}, \mathcal{E})$, The node homophily $h_{node}(v_i)$ quantifies the proportion of its labeled neighbors that share the same label y_{v_i} :

$$h_{node}(v_i) = \frac{|\{u | (u \in \mathcal{N}_{v_i} \cap \mathcal{V}_L) \text{ and } (y_{v_i} = y_u)\}|}{|\mathcal{N}_{v_i} \cap \mathcal{V}_L|}. \quad (1)$$

Definition 3.3. Accumulated Class Homophily. The accumulated class homophily for class c is defined as:

$$H(c) = \sum_{u \in \mathcal{N}_c^G} h_{node}(u), \quad (2)$$

where $\mathcal{N}_c^G = \{v_i \in \mathcal{V}_L | y_i = c\}$ represents the set of labeled nodes in G belonging to class c . Note that $H(c)$ considers both the quantity and topology of nodes. A higher $H(c)$ would indicate nodes of class c are numerous and exhibit strong homophily, making them more predictable for a vanilla graph model (Kipf & Welling, 2016).

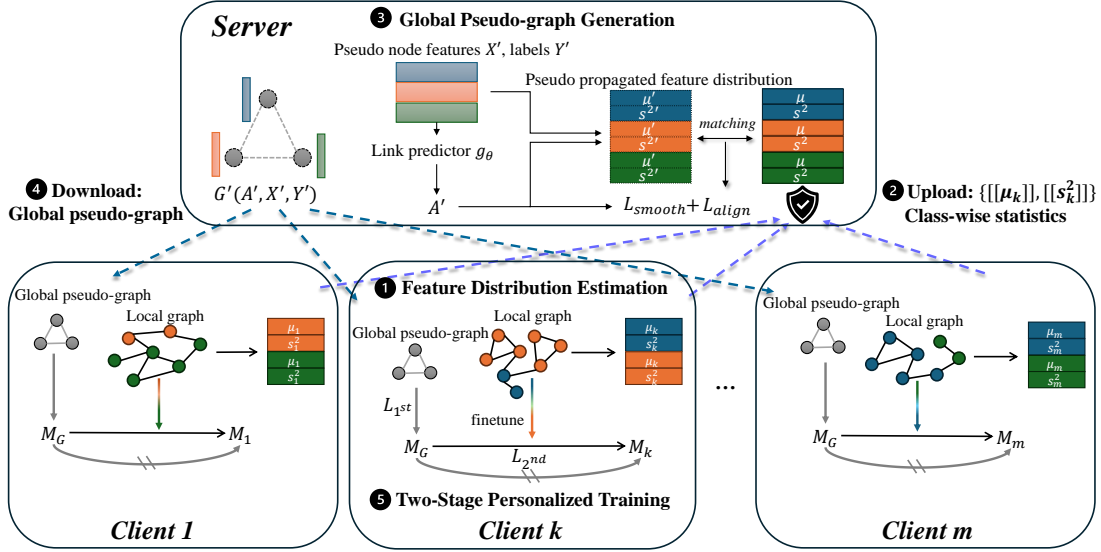
Definition 3.4. Class-aware Distillation Factor.

$$w_{dist}(c) = \frac{1}{1 + \log(H(c) + 1)}, \quad (3)$$

which can be organized into a vector $\mathbf{w}_{dist} \in \mathbb{R}^c$ where the i -th entry corresponds to $w_{dist}(i)$ for class i . \mathbf{w}_{dist} is used to determine γ_i for each node, as described in Section 4.4.

3.2. Problem Formulation

Assume a situation where a whole graph is distributed on m clients, each of which possesses its local non-overlapped


 Figure 3: The overall pipeline of our proposed method: **O-pFGL**.

subgraph. We formulate the one-shot personalized federated graph learning for node classification problem as:

$$\min \sum_{k=1}^m L(M_k(\mathbf{A}_k, \mathbf{X}_k), \mathbf{Y}_{k,U}), \quad (4)$$

This objective aims to minimize the aggregated generalization loss L on their unlabeled node set with personalized models M_k across all clients within a single upload-download communication round.

4. Proposed Method

4.1. Overall Pipeline

The overall pipeline of our method is illustrated in Figure 3, which comprises 5 steps. (1) Each client estimates the class-wise feature distribution and computes corresponding statistics on its local graph data; (2) Each client uploads its locally estimated class-wise statistics to the server; (3) The server aggregates the uploaded statistics by weighted average to recover the global class-wise feature distribution. Based on the recovered distribution, the server generates a small-size global pseudo-graph; (4) The server distributes the generated global pseudo-graph to clients; (5) Each client performs two-stage personalized training using both local graph data and the downloaded global pseudo-graph, deriving a model with improved personalization and generalization.

Specifically, in the first step, we propose a homophily-guided reliable node expansion strategy to augment the distribution estimation. In the third step, we adapt techniques from graph condensation to facilitate the global pseudo-graph generation. In the fifth step, we address the critical bias issue in personalization by proposing a two-stage per-

sonalized training process with node-adaptive distillation. The details are explained in the following sections.

4.2. Feature Distribution Estimation

To estimate the class-wise feature distribution locally, each client propagates node features on local graph data. Specifically, on client k , the propagated features are:

$$\mathbf{X}_k^{prop} = \parallel_{i=0}^h \tilde{\mathbf{A}}_k^i \mathbf{X}_k, \quad (5)$$

where h is the propagation depth and \parallel represents the concatenation. Using the propagated features, we unbiasedly estimate the sample mean and sample variance of features for labeled nodes in each class:

$$\begin{aligned} \mu_k^c &= \frac{1}{|\mathcal{V}_{k,L}^c|} \sum_{v_i \in \mathcal{V}_{k,L}^c} \mathbf{x}_i^{prop}, \\ s_k^{2c} &= \frac{1}{|\mathcal{V}_{k,L}^c| - 1} \sum_{v_i \in \mathcal{V}_{k,L}^c} (\mathbf{x}_i^{prop} - \mu_k^c)^2, \end{aligned} \quad (6)$$

where $\mathcal{V}_{k,L}^c$ denotes the labeled nodes of class c on client k . The statistics are estimated only for classes with sufficient labeled nodes, determined by a client-specified threshold.

However, due to the limited number of labeled nodes, the estimation may lack accuracy. To address this, we propose a Homophily-guided Reliable node Expansion (HRE) strategy as a plugin to further augment the estimation process on homophilic graphs. In HRE, we first apply Label Propagation (Iscen et al., 2019) to obtain the soft labels $\tilde{\mathbf{y}} \in \mathbb{R}^c$ for unlabeled nodes. We denote $c'_i = \arg \max_{0 \leq i < c} \tilde{\mathbf{y}}(i)$, then identify reliable soft labels based on the following criteria: (C1) **High Confidence**: $\tilde{\mathbf{y}}_i(c'_i) \geq f_{th}$; (C2) **High Class**

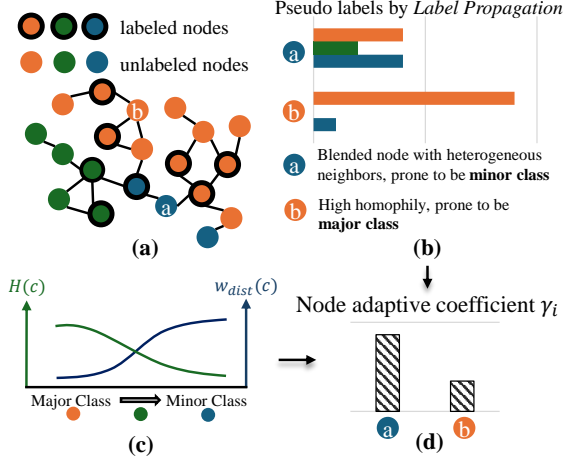


Figure 4: The process to determine γ_i for each node in node adaptive distillation in the second stage.

Homophily: $c'_i \in \text{top}K(H)$, indicating the node is likely to share the same label with its neighbors; **(C3) High Node Degree:** $d(v_i) \geq d_{th}$. A node with more neighbors could reduce the variance in predictions. With these criteria, the reliable nodes $\mathcal{V}_{k,r}$ set with inferred true labels is:

$$\mathcal{V}_{k,r} = \{v_i | (v_i \in \mathcal{V}_{k,U}) \wedge (\tilde{y}_i(c') \geq f_{th}) \wedge (d(v_i) \geq d_{th}) \wedge (c' \in \text{top}K(H))\}, \quad (7)$$

where $\text{top}K(H)$ is the set of classes corresponding to the top K largest values of accumulated class homophily $H(c)$. K , f_{th} and d_{th} are client-defined hyper-parameters. The reliable nodes $\mathcal{V}_{k,r}$, along with their inferred labels, can be used to expand the original labeled nodes set $\mathcal{V}_{k,L}$. The estimation of feature distribution could be augmented as:

$$\begin{aligned} \mu_k^c &= \frac{1}{|\mathcal{V}_{k,L}^c \cup \mathcal{V}_{k,r}^c|} \sum_{v_i \in \mathcal{V}_{k,L}^c \cup \mathcal{V}_{k,r}^c} \mathbf{x}_i^{prop}, \\ \mathbf{s}^{2^c}_k &= \frac{1}{|\mathcal{V}_{k,L}^c \cup \mathcal{V}_{k,r}^c| - 1} \sum_{v_i \in \mathcal{V}_{k,L}^c \cup \mathcal{V}_{k,r}^c} (\mathbf{x}_i^{prop} - \mu_k^c)^2, \end{aligned} \quad (8)$$

where $\mathcal{V}_{k,r}^c$ represents the subset of reliable nodes in $\mathcal{V}_{k,r}$ belonging to class c . This augmentation ensures a more accurate and robust estimation of class-wise feature distributions by incorporating reliable nodes into the computation.

4.3. Global Pseudo-Graph Generation

After clients estimate the class-wise feature distribution statistics $\{\mu_k^c, \mathbf{s}^{2^c}_k\}$, they upload them along with sample quantity of each class $\{N_k^c\}$ to the server. The server aggregates them to recover the global class-wise feature distribution. Specifically, the global mean and global variance of

class c are computed unbiasedly as:

$$\begin{aligned} N^c &= \sum_k N_k^c, \quad \mu^c = \frac{1}{N^c} \sum_k N_k^c \mu_k^c, \\ \mathbf{s}^{2^c} &= \frac{1}{N^c - m} \left(\sum_k (N_k^c - 1) \mathbf{s}^{2^c}_k + \sum_k N_k^c (\mu_k^c - \mu^c)^2 \right), \end{aligned} \quad (9)$$

which are used to guide the global pseudo-graph generation.

Inspired by the graph condensation (Liu et al., 2022; Xiao et al., 2024), we generate a small-size global pseudo-graph $G' = \{\mathbf{A}', \mathbf{X}', \mathbf{Y}'\}$ by aligning its feature distribution with the aggregated global distribution. This pseudo-graph serves as a representative of the overall graph data across all clients. The generation process is illustrated in the top of Figure 3. We firstly pre-set the number of nodes of each class in the pseudo-graph and initialize the trainable node features \mathbf{X}' from Gaussian noise. The adjacency matrix \mathbf{A}' is defined using a trainable link predictor g_θ :

$$\mathbf{A}'_{i,j} = g_\theta(\mathbf{X}', \delta) = \mathbb{I}(\delta \leq \sigma(\frac{g_\theta(\mathbf{x}_i \| \mathbf{x}_j) + g_\theta(\mathbf{x}_j \| \mathbf{x}_i)}{2})), \quad (10)$$

where σ denotes Sigmoid function, δ is a hyper-parameter to control sparsity, and \parallel represents concatenation.

Following (Xiao et al., 2024), to optimize \mathbf{X}' and g_θ , we first propagate node features \mathbf{X}' as in Eq. 5. Then we calculate the class-wise sample mean μ^c and sample variance \mathbf{s}^{2^c} of the propagated node features \mathbf{X}'^{prop} following Eq. 6. Then we calculate the alignment loss:

$$L_{align} = \sum_{c=0}^{C-1} \lambda_c ((\mu^c - \mu^c)^2 + (\mathbf{s}^{2^c} - \mathbf{s}^{2^c})^2), \quad (11)$$

where λ_c is the proportion of nodes belonging to class c relative to the total number of nodes. To ensure the smoothness of the pseudo-graph, smoothness loss is applied:

$$L_{smt} = \frac{1}{\sum_{i,j} \mathbf{A}'_{i,j}} \sum_{i,j} \mathbf{A}'_{i,j} \exp(-\frac{\|\mathbf{x}_i - \mathbf{x}_j\|^2}{2}). \quad (12)$$

We could optimize the \mathbf{X}' and g_θ to generate the global pseudo-graph by the overall optimization objective:

$$\min_{\mathbf{X}', \theta} (L_{align} + \alpha L_{smt}). \quad (13)$$

Once the global pseudo-graph is generated, the server distributes it to clients for further personalized training.

Privacy-preservation with Secure Aggregation. We demonstrate compatibility with Secure Aggregation protocols in uploading and aggregating $\{\mu_k^c, \mathbf{s}^{2^c}_k, N_k^c\}$. Secure Aggregation enables the server to compute the sum of large, user-held data vectors securely, without accessing individual client contributions. This property aligns well with the

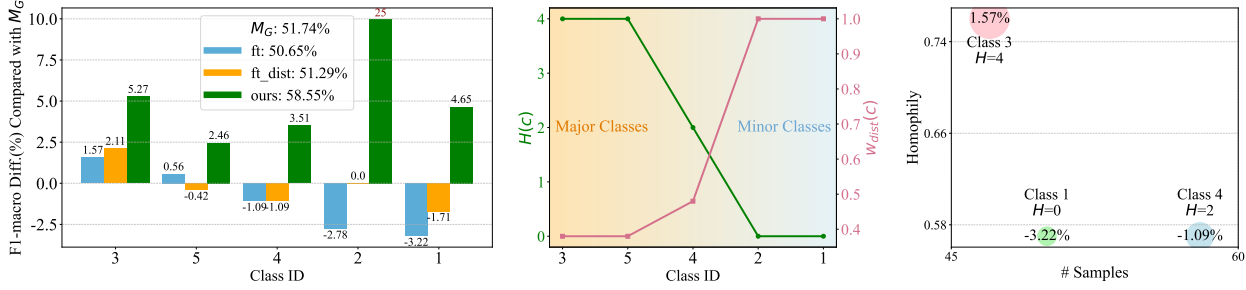


Figure 5: Analysis of a client on the CiteSeer dataset. **Left:** The performance difference of our method (ours) and two variants (ft and ft_dist) compared with M_G trained solely on the global pseudo-graph. **Middle:** The value of H and w_{dist} of each class. **Right:** The value of H is influenced by both the number of samples and their homophily.

aggregation process in Eq. 9, as it can be expressed as a series of weighted average operations. The calculation of N^c and μ^c are inherently weighted averages. The calculation of s^{2^c} , while more complex, can also be decomposed into weighted average operations:

$$s^{2^c} = \frac{\sum_k^m (N_k^c - 1) s_k^{2^c}}{N^c - m} + \frac{\sum_k^m N_k^c (\mu_k^c)^2 - 2\mu^c \sum_k^m \mu_k^c + N^c \sum_k^m (\mu^c)^2}{N^c - m}. \quad (14)$$

Breaking this down further, the calculation involves the weighted averages of $(N_k^c - 1) s_k^{2^c}$, $N_k^c (\mu_k^c)^2$ and μ_k^c . Thus, the entire aggregation process for $\{\mu_k^c, s_k^{2^c}, N_k^c\}$ can be conducted without revealing individual client data contributions, making it fully compatible with Secure Aggregation.

4.4. Personalized Training with Node Adaptive Distillation

With the downloaded global pseudo-graph, each client trains its personalized model locally. However, the imbalanced local graph data often results in biased models that perform well on major classes but neglect minor classes. To achieve better personalization (high accuracy) and generalization (high F1-macro), we propose a two-stage adaptive personalized training approach with node-adaptive distillation to leverage both the global information in the global pseudo-graph and personal information in the local data.

Stage 1 Each client trains a local model M_G using only the global pseudo-graph, ensuring M_G to capture global, balanced knowledge. The training objective is to minimize:

$$L_{1st} = L_{ce}(M_G(\mathbf{A}', \mathbf{X}'), \mathbf{Y}'). \quad (15)$$

A copy of the resulting M_G is detached as a fixed teacher model for the next stage. L_{ce} denotes the cross-entropy loss.

Stage 2 Client k fine-tunes M_G with local graph data to derive a personalized model M_k . However, fine-tuning on

imbalanced local graph data often leads to over-fitting on major classes while forgetting minor classes. As illustrated in Figure 5, the fine-tuned model shows improvement in major classes but suffers degradation in minor classes.

To mitigate this, we propose to utilize the global knowledge of M_G and personalized knowledge in local graph data to train a better M_k with the node adaptive distillation. For nodes of major classes, the model directly learns through supervised fine-tuning. For nodes of minor classes, M_k additionally distills the predictive ability from M_G . The training objective for the second stage is to minimize:

$$L_{2nd} = L_{ft} + L_{dist}, \quad (16)$$

where L_{ft} is the cross-entropy loss for supervised fine-tuning on local training data, and L_{dist} is the weighted sum of point-wise KL divergence loss to distill global knowledge from M_G into M_k :

$$L_{dist} = \sum_{\mathbf{x}_i \in \mathbf{X}_k} \gamma_i L_{kl}(M_k(\mathbf{A}_k, \mathbf{x}_i), M_G(\mathbf{A}_k, \mathbf{x}_i)), \quad (17)$$

γ_i is a node-specific weighting factor that controls the balance between local fine-tuning and global knowledge distillation. To determine γ_i for each node, we utilize the soft labels $\tilde{\mathbf{y}}_i$ obtained in Section 4.2 and \mathbf{w}_{dist} in Eq. 3:

$$\gamma_i = \beta \tilde{\mathbf{y}}_i \cdot \mathbf{w}_{dist}, \quad (18)$$

where β is a scaling hyper-parameter. Intuitively explained, if a node is predicted to class c with a small $w_{dist}(c)$ (e.g. node b in Figure 4), it likely belongs to major classes with high homophily. In this case, γ_i is small, and M_i primarily learns through supervised fine-tuning; If a node is predicted to class c with a large $w_{dist}(c)$ or has a blended prediction (e.g. node a in Figure 4), it likely belongs to minor classes or has low homophily. These nodes are often neglected during supervised fine-tuning. Thus γ_i should be large to incorporate corresponding global knowledge from M_G .

Table 1: Performance on datasets under Louvain partition with 10 clients. OOM represents the out-of-memory issue.

Method	Cora		CiteSeer		PubMed		ogbn-arxiv		ogbn-products	
	Acc.	F1								
Standalone	67.17 \pm 0.38	41.79 \pm 0.52	59.82 \pm 0.12	42.70 \pm 0.34	81.74 \pm 0.06	64.61 \pm 0.18	66.46 \pm 0.24	16.59 \pm 0.57	85.25 \pm 0.02	22.35 \pm 0.19
FedAvg	69.68 \pm 0.48	45.10 \pm 0.75	63.92 \pm 0.10	45.97 \pm 0.43	78.24 \pm 0.08	42.24 \pm 0.13	67.13 \pm 0.14	18.46 \pm 0.23	85.34 \pm 0.04	22.80 \pm 0.04
FedPUB	68.50 \pm 0.38	43.35 \pm 0.27	61.80 \pm 0.37	43.96 \pm 1.05	81.63 \pm 0.54	63.39 \pm 0.69	65.34 \pm 0.28	12.50 \pm 0.20	83.91 \pm 0.31	17.29 \pm 0.52
FedGTA	42.61 \pm 0.76	23.47 \pm 1.06	67.12 \pm 1.58	52.68 \pm 1.81	75.99 \pm 1.21	57.48 \pm 1.44	58.30 \pm 0.30	12.22 \pm 0.26	75.87 \pm 0.04	16.58 \pm 0.15
FedTAD	70.10 \pm 0.22	45.57 \pm 0.27	63.93 \pm 0.27	44.59 \pm 0.41	78.21 \pm 0.31	42.45 \pm 0.80	68.77 \pm 0.12	27.33 \pm 0.50	OOM	OOM
FedSpray	63.14 \pm 1.73	40.82 \pm 1.54	54.89 \pm 4.24	39.56 \pm 3.58	77.89 \pm 1.67	64.23 \pm 2.03	68.68 \pm 0.05	19.90 \pm 0.16	84.06 \pm 0.11	20.80 \pm 0.05
DENSE	69.89 \pm 0.30	45.35 \pm 0.55	64.09 \pm 0.48	46.00 \pm 0.39	78.16 \pm 0.06	41.96 \pm 0.33	68.80 \pm 0.04	27.60 \pm 0.36	86.12 \pm 0.03	26.58 \pm 0.06
Co-Boost	69.95 \pm 0.40	45.43 \pm 0.52	64.21 \pm 0.27	46.00 \pm 0.11	78.13 \pm 0.05	41.84 \pm 0.22	66.27 \pm 0.08	16.37 \pm 0.14	85.24 \pm 0.00	22.31 \pm 0.11
O-pFGL (Ours)	76.43 \pm 1.24	61.58 \pm 2.16	71.61 \pm 0.40	58.24 \pm 0.96	82.71 \pm 0.03	66.40 \pm 0.34	70.93 \pm 0.59	36.66 \pm 0.22	86.63 \pm 0.02	27.21 \pm 0.15

5. Experiments

5.1. Experimental Setup

Datasets. We conduct our experiments on 12 datasets considering both transductive and inductive learning settings. For the transductive setting, we use Cora, CiteSeer, and PubMed from (Yang et al., 2016) and ogbn-arxiv and ogbn-products (Hu et al., 2020). We also use Computers, Photo, CS, Physics datasets (Shchur et al., 2018). For the inductive setting, we use Flickr (Zeng et al., 2019), Reddit (Hamilton et al., 2017), and Reddit2 (Zeng et al., 2019). A summary of these datasets is provided in Table 4 in the Appendix. To simulate distributed subgraphs, we employ two advanced graph partitions: Louvain-based Label Imbalance Split and Metis-based Label Imbalance Split (Li et al., 2024c).

Baselines. We compare our method with 8 state-of-the-art methods including 4 pFGL methods¹: (1) FedPUB (Baek et al., 2023), (2) FedGTA (Li et al., 2024b), (3) FedTAD (Zhu et al., 2024b), (4) FedSpray (Fu et al., 2024), which pays attention to minority, and 2 OFL methods: (5) DENSE (Zhang et al., 2022), (6) Co-Boost (Dai et al., 2024). We also include (7) Standalone, which locally trains models, and (8) FedAvg with fine-tuning, as additional baselines.

Metrics. We employ both accuracy(%) and F1-macro(%) metrics. F1-macro averages F1 score across all classes, providing a more robust measurement of the model’s generalization, particularly under imbalanced data. we report the mean and standard deviation across three runs.

Hyper-parameters and Configurations. We limit the communication round to a single round. We employ the two-layer GCN (Kipf & Welling, 2016) with the hidden dimension set to 64. Detailed settings and configurations under model heterogeneity are described in the Appendix.

¹We do not include FedSage (Zhang et al., 2021) and AdaFGL (Li et al., 2024a) since they need extra communication rounds to train neighborhood generators or federated optimization. They cannot train models within one-shot communication.

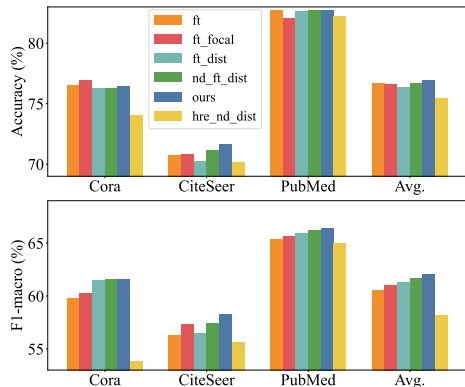


Figure 6: Ablation study under Louvain partition.

5.2. Experimental Results

5.2.1. PERFORMANCE COMPARISON

The performance under the Louvain partition with 10 clients is shown in Table 1 and results with more clients and under the Metis partition are in the Appendix. Our method consistently outperforms on both accuracy and F1-macro, demonstrating the superiority of our method in deriving models with better personalization and local generalization. FedTAD encounters the OOM issue due to its graph diffusion operation. FedSpray focuses on minor classes, but it requires numerous communication for optimization, offering little advantage in one-shot communication. Furthermore, our method even generally outperforms other methods with 100 communication rounds, which is shown in Section A.2.2 in Appendix. More results on Computers, Photo, CS, and Physics datasets are also listed in Appendix.

5.2.2. ABLATION STUDY

We conduct the ablation study to analysis our method. We compare our method with 5 variants: (1) ft: only fine-tuning M_G to obtain M_i on local graph data, (2) ft_focal: fine-tuning with focal loss (Ross & Dollár, 2017) to handle data imbalance, (3) ft_dist: in the second stage, performing distil-

Table 2: Performance of methods on inductive datasets.

Method	Flickr		Reddit		Reddit2	
	Acc.	F1	Acc.	F1	Acc.	F1
Standalone	44.97 \pm 0.70	12.84 \pm 0.06	90.35 \pm 0.02	28.79 \pm 0.07	91.92 \pm 0.01	32.53 \pm 0.20
FedAvg	45.50 \pm 0.97	13.66 \pm 0.20	80.75 \pm 0.81	16.85 \pm 0.49	82.86 \pm 0.62	19.20 \pm 0.44
FedPUB	42.17 \pm 0.00	8.32 \pm 0.00	90.74 \pm 0.02	27.86 \pm 0.01	92.03 \pm 0.02	30.37 \pm 0.09
FedGTA	29.99 \pm 1.71	14.38 \pm 1.15	90.35 \pm 0.02	28.76 \pm 0.24	91.91 \pm 0.38	32.71 \pm 0.11
FedTAD	45.44 \pm 0.47	13.85 \pm 0.50	OOM			
FedSpray	43.08 \pm 0.32	13.08 \pm 1.75	89.07 \pm 0.21	27.28 \pm 0.24	91.28 \pm 0.11	31.90 \pm 0.17
DENSE	44.60 \pm 0.28	12.47 \pm 0.39	90.32 \pm 0.04	30.08 \pm 0.10	92.00 \pm 0.05	34.42 \pm 0.29
Co-Boost	45.79 \pm 0.54	13.52 \pm 0.52	90.35 \pm 0.03	28.62 \pm 0.05	91.94 \pm 0.02	32.68 \pm 0.04
O-pFGL (Ours)	46.83 \pm 0.44	14.31 \pm 0.04	90.74 \pm 0.11	30.09 \pm 0.49	92.14 \pm 0.05	35.51 \pm 0.15

Table 3: Performance with heterogeneous models.

Louvain	Cora		CiteSeer		ogbn-arxiv	
	Acc.	F1	Acc.	F1	Acc.	F1
Standalone	68.37 \pm 0.19	43.51 \pm 0.31	62.50 \pm 0.15	43.94 \pm 0.09	66.13 \pm 0.08	19.60 \pm 0.38
FedTAD	68.18 \pm 0.22	42.91 \pm 0.34	61.81 \pm 0.18	43.78 \pm 0.14	69.08 \pm 0.08	29.29 \pm 0.44
FedSpray	65.73 \pm 1.05	42.23 \pm 0.34	53.14 \pm 1.19	39.13 \pm 1.17	68.63 \pm 0.03	22.25 \pm 0.26
DENSE	68.15 \pm 0.47	43.02 \pm 0.36	62.31 \pm 0.51	44.27 \pm 0.44	69.03 \pm 0.02	29.64 \pm 0.14
Co-Boost	68.38 \pm 0.40	43.13 \pm 0.52	62.22 \pm 0.18	44.23 \pm 0.05	69.08 \pm 0.13	29.88 \pm 0.27
O-pFGL (Ours)	75.04 \pm 0.50	57.26 \pm 1.93	70.87 \pm 0.21	56.67 \pm 0.20	70.98 \pm 0.09	36.41 \pm 0.43

lation on all nodes with a fixed γ_i ; (4) `nd_ft_dist`: performing node adaptive distillation along with fine-tuning, without HRE, (5) `ours`: performing the complete method (including HRE), and (6) `hre_nd_dist`: performing our complete method but without the first stage in personalized training, instead train a model from scratch in the second stage.

The results under the Louvain partition and Metis partition are shown in Figure 6 and Figure 8 in the Appendix, respectively. The focal loss cannot effectively address the non-IID graph data since it’s hard to determine the proper weights. Fixed distillation cannot balance improvements in accuracy and F1 macro as it does not distinguish the majority from the minority. For nodes in major classes, the global knowledge of M_G may have a negative impact, as demonstrated by the left sub-figure in Figure 5. This motivates us to develop node-adaptive distillation. The node adaptive distillation is more flexible to determine when to introduce the global knowledge of M_G in fine-tuning. And the HRE strategy further improves performance by generating a better global pseudo-graph with more precise estimations. Comparing `ours` and `hre_nd_dist`, we conclude that M_G provides a necessary start-point for fine-tuning. Furthermore, We justify the rationale for considering homophily in determining the major classes by H values in Eq. 2 in the right panel of Figure 5. The full analysis is in the Appendix.

5.2.3. PERFORMANCE UNDER MODEL HETEROGENEITY

We conduct experiments on 10 clients with heterogeneous models. Under model heterogeneity, most pFGL methods do not work since they rely on the model parameter aggregation. The results under Louvain and Metis partitions are presented in Table 3 and Table 11 in the Appendix, respectively. The results demonstrate the superior performance of our method

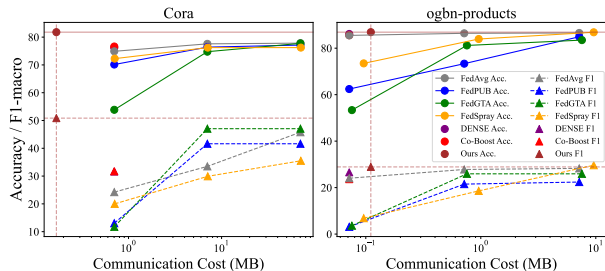


Figure 7: Communication costs versus performance.

in both accuracy and F1-macro.

5.2.4. INDUCTIVE PERFORMANCE

The results on inductive graph datasets under the Louvain partition are shown in Table 2 and more results are shown in the Appendix. Since Flickr has lower homophily, we use 2-layer SIGN (Frasca et al., 2020) for better graph learning. Our method is scalable and generally performs best.

5.2.5. COMMUNICATION ANALYSIS

We analyze the communication costs both theoretically and empirically. Our method involves uploading the class-wise statistics ($O(Chf)$) and downloading the generated global pseudo-graph ($O(n'f + n'^2)$, where n' is the number of nodes in the global pseudo-graph). Both communications are independent of the model size. Figure 7 reports the communication costs of uploading and downloading on a client on small-scale Cora and large-scale ogbn-products graph datasets under the Metis partition. Note that we report the performance and costs of 1, 10, and 100 communication rounds for FedAvg, FedPUB, FedGTA, and FedSpray. The results demonstrate that our method achieves better performance with lower communication costs. Detailed analysis of *communication*, *computation*, and *memory* is shown in Table 19, Table 20, and Table 21 in the Appendix.

6. Conclusion

We propose the first one-shot personalized federated graph learning method that supports model heterogeneity and Secure Aggregation. Specifically, our method first estimates class-wise feature distribution statistics on each client, augmented by our proposed HRE, and then aggregates these statistics on the server to generate the global pseudo-graph. To further enhance personalization and generalization, we propose a novel two-stage personalized training with node-adaptive distillation, which balances local information and global insights. Extensive experiments demonstrate the superior performance of our method across various settings.

Impact Statement

This paper presents work whose goal is to advance the field of Machine Learning. There are many potential societal consequences of our work, none which we feel must be specifically highlighted here.

References

- Acar, A., Aksu, H., Uluagac, A. S., and Conti, M. A survey on homomorphic encryption schemes: Theory and implementation. *ACM Computing Surveys (Csur)*, 51(4):1–35, 2018.
- Baek, J., Jeong, W., Jin, J., Yoon, J., and Hwang, S. J. Personalized subgraph federated learning. In *International conference on machine learning*, pp. 1396–1415. PMLR, 2023.
- Bang, D., Lim, S., Lee, S., and Kim, S. Biomedical knowledge graph learning for drug repurposing by extending guilt-by-association to multiple layers. *Nature Communications*, 14(1):3570, 2023.
- Bonawitz, K., Ivanov, V., Kreuter, B., Marcedone, A., McMahan, H. B., Patel, S., Ramage, D., Segal, A., and Seth, K. Practical secure aggregation for privacy-preserving machine learning. In *proceedings of the 2017 ACM SIGSAC Conference on Computer and Communications Security*, pp. 1175–1191, 2017.
- Chen, D., Lin, Y., Zhao, G., Ren, X., Li, P., Zhou, J., and Sun, X. Topology-imbalance learning for semi-supervised node classification. *Advances in Neural Information Processing Systems*, 34:29885–29897, 2021.
- Dai, R., Shen, L., He, F., Tian, X., and Tao, D. Dispf: Towards communication-efficient personalized federated learning via decentralized sparse training. In *International conference on machine learning*, pp. 4587–4604. PMLR, 2022.
- Dai, R., Zhang, Y., Li, A., Liu, T., Yang, X., and Han, B. Enhancing one-shot federated learning through data and ensemble co-boosting. *arXiv preprint arXiv:2402.15070*, 2024.
- Frasca, F., Rossi, E., Eynard, D., Chamberlain, B., Bronstein, M., and Monti, F. Sign: Scalable inception graph neural networks. *arXiv preprint arXiv:2004.11198*, 2020.
- Fu, X., Zhang, B., Dong, Y., Chen, C., and Li, J. Federated graph machine learning: A survey of concepts, techniques, and applications. *ACM SIGKDD Explorations Newsletter*, 24(2):32–47, 2022.
- Fu, X., Chen, Z., Zhang, B., Chen, C., and Li, J. Federated graph learning with structure proxy alignment. In *Proceedings of the 30th ACM SIGKDD Conference on Knowledge Discovery and Data Mining*, pp. 827–838, 2024.
- Gasteiger, J., Bojchevski, A., and Günnemann, S. Predict then propagate: Graph neural networks meet personalized pagerank. *arXiv preprint arXiv:1810.05997*, 2018.
- Gu, Z., Zhang, K., Bai, G., Chen, L., Zhao, L., and Yang, C. Dynamic activation of clients and parameters for federated learning over heterogeneous graphs. In *2023 IEEE 39th International Conference on Data Engineering (ICDE)*, pp. 1597–1610. IEEE, 2023.
- Guha, N., Talwalkar, A., and Smith, V. One-shot federated learning. *arXiv preprint arXiv:1902.11175*, 2019.
- Hamilton, W., Ying, Z., and Leskovec, J. Inductive representation learning on large graphs. *Advances in neural information processing systems*, 30, 2017.
- He, L., Wang, X., Wang, D., Zou, H., Yin, H., and Xu, G. Simplifying graph-based collaborative filtering for recommendation. In *Proceedings of the sixteenth ACM international conference on web search and data mining*, pp. 60–68, 2023.
- Heinbaugh, C. E., Luz-Ricca, E., and Shao, H. Data-free one-shot federated learning under very high statistical heterogeneity. In *The Eleventh International Conference on Learning Representations*, 2023.
- Hu, W., Fey, M., Zitnik, M., Dong, Y., Ren, H., Liu, B., Catasta, M., and Leskovec, J. Open graph benchmark: Datasets for machine learning on graphs. *Advances in neural information processing systems*, 33:22118–22133, 2020.
- Hyun, W., Lee, J., and Suh, B. Anti-money laundering in cryptocurrency via multi-relational graph neural network. In *Pacific-Asia Conference on Knowledge Discovery and Data Mining*, pp. 118–130. Springer, 2023.
- Iscen, A., Tolia, G., Avrithis, Y., and Chum, O. Label propagation for deep semi-supervised learning. In *Proceedings of the IEEE/CVF conference on computer vision and pattern recognition*, pp. 5070–5079, 2019.
- Kairouz, P., McMahan, H. B., Avent, B., Bellet, A., Bennis, M., Bhagoji, A. N., Bonawitz, K., Charles, Z., Cormode, G., Cummings, R., et al. Advances and open problems in federated learning. *Foundations and trends® in machine learning*, 14(1–2):1–210, 2021.
- Kipf, T. N. and Welling, M. Semi-supervised classification with graph convolutional networks. *arXiv preprint arXiv:1609.02907*, 2016.

- Li, X., Wu, Z., Zhang, W., Sun, H., Li, R.-H., and Wang, G. Adafgl: A new paradigm for federated node classification with topology heterogeneity. *arXiv preprint arXiv:2401.11750*, 2024a.
- Li, X., Wu, Z., Zhang, W., Zhu, Y., Li, R.-H., and Wang, G. Fedgta: Topology-aware averaging for federated graph learning. *arXiv preprint arXiv:2401.11755*, 2024b.
- Li, X., Zhu, Y., Pang, B., Yan, G., Yan, Y., Li, Z., Wu, Z., Zhang, W., Li, R.-H., and Wang, G. Openfgl: A comprehensive benchmarks for federated graph learning. *arXiv preprint arXiv:2408.16288*, 2024c.
- Liu, M., Li, S., Chen, X., and Song, L. Graph condensation via receptive field distribution matching. *arXiv preprint arXiv:2206.13697*, 2022.
- Mothukuri, V., Parizi, R. M., Pouriyeh, S., Huang, Y., Dehghantaha, A., and Srivastava, G. A survey on security and privacy of federated learning. *Future Generation Computer Systems*, 115:619–640, 2021.
- Pan, Q., Zhu, Y., and Chu, L. Lumos: Heterogeneity-aware federated graph learning over decentralized devices. In *2023 IEEE 39th International Conference on Data Engineering (ICDE)*, pp. 1914–1926. IEEE, 2023.
- Rombach, R., Blattmann, A., Lorenz, D., Esser, P., and Ommer, B. High-resolution image synthesis with latent diffusion models. In *Proceedings of the IEEE/CVF conference on computer vision and pattern recognition*, pp. 10684–10695, 2022.
- Ross, T.-Y. and Dollár, G. Focal loss for dense object detection. In *proceedings of the IEEE conference on computer vision and pattern recognition*, pp. 2980–2988, 2017.
- Shchur, O., Mumme, M., Bojchevski, A., and Günnemann, S. Pitfalls of graph neural network evaluation. *arXiv preprint arXiv:1811.05868*, 2018.
- So, J., He, C., Yang, C.-S., Li, S., Yu, Q., E Ali, R., Guler, B., and Avestimehr, S. Lightsecagg: a lightweight and versatile design for secure aggregation in federated learning. *Proceedings of Machine Learning and Systems*, 4: 694–720, 2022.
- Song, R., Liu, D., Chen, D. Z., Festag, A., Trinitis, C., Schulz, M., and Knoll, A. Federated learning via decentralized dataset distillation in resource-constrained edge environments. In *2023 International Joint Conference on Neural Networks (IJCNN)*, pp. 1–10. IEEE, 2023.
- Tan, Y., Liu, Y., Long, G., Jiang, J., Lu, Q., and Zhang, C. Federated learning on non-iid graphs via structural knowledge sharing. In *Proceedings of the AAAI conference on artificial intelligence*, volume 37, pp. 9953–9961, 2023.
- Veličković, P., Cucurull, G., Casanova, A., Romero, A., Lio, P., and Bengio, Y. Graph attention networks. *arXiv preprint arXiv:1710.10903*, 2017.
- Wang, D., Li, C., Wen, S., Nepal, S., and Xiang, Y. Man-in-the-middle attacks against machine learning classifiers via malicious generative models. *IEEE Transactions on Dependable and Secure Computing*, 18(5):2074–2087, 2020.
- Wu, F., Souza, A., Zhang, T., Fifty, C., Yu, T., and Weinberger, K. Simplifying graph convolutional networks. In *International conference on machine learning*, pp. 6861–6871. PMLR, 2019.
- Wu, Z., Pan, S., Chen, F., Long, G., Zhang, C., and Philip, S. Y. A comprehensive survey on graph neural networks. *IEEE transactions on neural networks and learning systems*, 32(1):4–24, 2020.
- Xiao, Z., Wang, Y., Liu, S., Wang, H., Song, M., and Zheng, T. Simple graph condensation. In *Joint European Conference on Machine Learning and Knowledge Discovery in Databases*, pp. 53–71. Springer, 2024.
- Xie, H., Ma, J., Xiong, L., and Yang, C. Federated graph classification over non-iid graphs. *Advances in neural information processing systems*, 34:18839–18852, 2021.
- Yang, M., Su, S., Li, B., and Xue, X. Exploring one-shot semi-supervised federated learning with pre-trained diffusion models. In *Proceedings of the AAAI Conference on Artificial Intelligence*, volume 38, pp. 16325–16333, 2024a.
- Yang, M., Su, S., Li, B., and Xue, X. Feddeo: Description-enhanced one-shot federated learning with diffusion models. *arXiv preprint arXiv:2407.19953*, 2024b.
- Yang, Z., Cohen, W., and Salakhudinov, R. Revisiting semi-supervised learning with graph embeddings. In *International conference on machine learning*, pp. 40–48. PMLR, 2016.
- Zeng, H., Zhou, H., Srivastava, A., Kannan, R., and Prasanna, V. Graphsaint: Graph sampling based inductive learning method. *arXiv preprint arXiv:1907.04931*, 2019.
- Zhang, J., Chen, C., Li, B., Lyu, L., Wu, S., Ding, S., Shen, C., and Wu, C. Dense: Data-free one-shot federated learning. *Advances in Neural Information Processing Systems*, 35:21414–21428, 2022.
- Zhang, K., Yang, C., Li, X., Sun, L., and Yiu, S. M. Sub-graph federated learning with missing neighbor generation. *Advances in Neural Information Processing Systems*, 34:6671–6682, 2021.

- Zhang, K., Sun, L., Ding, B., Yiu, S. M., and Yang, C. Deep efficient private neighbor generation for subgraph federated learning. In *Proceedings of the 2024 SIAM International Conference on Data Mining (SDM)*, pp. 806–814. SIAM, 2024.
- Zhou, Y., Pu, G., Ma, X., Li, X., and Wu, D. Distilled one-shot federated learning. *arXiv preprint arXiv:2009.07999*, 2020.
- Zhu, G., Li, D., Gu, H., Han, Y., Yao, Y., Fan, L., and Yang, Q. Evaluating membership inference attacks and defenses in federated learning. *arXiv preprint arXiv:2402.06289*, 2024a.
- Zhu, H. and Koniusz, P. Simple spectral graph convolution. In *International conference on learning representations*, 2021.
- Zhu, Y., Li, X., Wu, Z., Wu, D., Hu, M., and Li, R.-H. Fedtad: Topology-aware data-free knowledge distillation for subgraph federated learning. *arXiv preprint arXiv:2404.14061*, 2024b.

A. Appendix

A.1. Experimental Setup

Table 4: The statistics and description of the datasets.

Dataset	Task	#Nodes	#Edges	#Features	#Classes	Train/Val/Test	Description
Cora	Transductive	2,708	10,556	1433	7	20%/40%/40%	Citation Network
CiteSeer	Transductive	3,327	4,732	3703	6	20%/40%/40%	Citation Network
PubMed	Transductive	19,717	44,338	500	3	20%/40%/40%	Citation Network
Ogbn-arxiv	Transductive	169,343	1,166,243	128	40	60%/20%/20%	Citation Network
Ogbn-products	Transductive	2,449,029	61,859,140	100	47	10%/5%/85%	Co-purchase Network
Computers	Transductive	13,381	245,778	767	10	20%/40%/40%	Co-purchase Network
Photo	Transductive	7,487	119,043	745	8	20%/40%/40%	Co-purchase Network
CS	Transductive	18,333	81,894	6,805	15	20%/40%/40%	Co-author Network
Physics	Transductive	34,493	247,962	8,415	5	20%/40%/40%	Co-author Network
Flickr	Inductive	89,250	899,756	500	7	60%/20%/20%	Image Network
Reddit	Inductive	232,965	114,615,892	602	41	80%/10%/10%	Social Network
Reddit2	Inductive	232,965	23,213,838	602	41	65%/10%/25%	Social Network

Dataset Description We conduct experiments on 12 graph datasets and the summary is listed in Table 4. Our selected datasets cover a wide range from 1) small-scale to large-scale, 2) transductive to inductive, and 3) academic domain to industry domain.

Additional Baselines Description In DENSE and Co-Boost, the generators are trained to generate node features, and the topology structure is constructed using the K -Nearest Neighbors strategy as outlined in (Zhu et al., 2024b). Note that we perform additional fine-tuning processes on FedTAD, DENSE, and Co-Boost to ensure better performance.

Hyper-parameters and Model Configurations In our one-shot personalized federated graph learning setting, we limit the communication round to a single round. For each client, we employ a two-layer GCN (Kipf & Welling, 2016) with the hidden layer dimension set to 64 by default. For baseline methods, the number of local training epochs is tuned from 3 to 100, and hyper-parameters are set as recommended in their respective papers or fine-tuned for optimal overall performance. For our method, we keep the size of the generated global pseudo-graph as small as possible. On small-scale Cora, CiteSeer and PubMed datasets, we set the number of nodes in each class in the global pseudo-graph as 1. We set p as 0.25%, 0.04%, 1%, 1%, 1%, 0.5%, 0.2%, 0.05%, 0.05% on ogbn-arxiv, ogbn-products, Computers, Photo, CS, Physics, Flickr, Reddit, and Reddit2 datasets. We tune f_{th} within [0.95, 1] and tune d_{th} according to the scale of the graphs. We tune the β within [0.1, 1] to control the range of γ_i . For other hyper-parameters in global pseudo-graph generation, we adopt the setting in (Xiao et al., 2024). Under model heterogeneity, we adopt 10 different GNN models categorized into two types: coupled GNNs and decoupled GNNs. For coupled GNNs, we adopt 6 models which are: 2-layer GCN with 64, 128, 256, and 512 hidden dimension, 3-layer GCN with 64 and 512 hidden dimension. For decoupled GNNs, we adopt APPNP (Gasteiger et al., 2018), SSGC (Zhu & Koniusz, 2021), SGC ($K=2$) and SGC ($K=4$) (Wu et al., 2019).

Experimental Environments The experimental machine is with Intel(R) Xeon(R) CPU E5-2680 v4@2.40GHz, and 6×NVIDIA GeForce RTX 3090. The operating system is Ubuntu 20.04 and the version of PyTorch is 2.1.2.

A.2. More Experimental Results and Full Analysis

A.2.1. PERFORMANCE COMPARISON

We first conduct experiments in the transductive learning setting and report the accuracy and F1-macro metrics. The datasets range from small-scale graphs to large-scale graphs with millions of nodes. We also varies the number of clients to evaluate the stability of methods. With 10 clients, the experimental results under Louvain and Metis partitions are shown in Table 1 and Table 6, respectively. With 20 clients, the experimental results under Louvain and Metis partitions are shown in Table 5 and Table 8, respectively. Our method consistently outperforms others in terms of accuracy and F1-macro. Under the non-IID scenarios, pFGL methods show marginal or even negative performance gain over Standalone, highlighting the ineffectiveness of current pFGL methods in personalizing models on non-IID graph data in a single communication round.

Table 5: Performance of methods on datasets under Louvain partition with 20 clients.

Method	Cora		CiteSeer		PubMed		ogbn-arxiv		ogbn-products	
	Acc.	F1								
Standalone	61.57 \pm 0.84	30.35 \pm 0.59	57.86 \pm 0.62	36.44 \pm 0.52	81.84 \pm 0.04	57.95 \pm 0.62	66.56 \pm 0.16	13.53 \pm 0.34	86.44 \pm 0.01	17.34 \pm 0.05
FedAvg	63.21 \pm 0.45	31.77 \pm 0.64	61.51 \pm 0.27	40.60 \pm 0.40	78.59 \pm 0.14	41.60 \pm 0.28	67.17 \pm 0.12	15.33 \pm 0.44	86.48 \pm 0.01	17.57 \pm 0.12
FedPUB	62.52 \pm 0.27	30.96 \pm 0.25	59.40 \pm 0.29	37.59 \pm 0.19	81.41 \pm 0.14	56.81 \pm 1.94	65.83 \pm 0.33	10.32 \pm 0.53	83.47 \pm 1.18	11.23 \pm 0.74
FedGTA	37.03 \pm 1.34	14.74 \pm 0.76	62.02 \pm 0.83	42.78 \pm 0.92	64.01 \pm 0.98	36.47 \pm 1.33	57.59 \pm 1.39	7.72 \pm 0.67	79.04 \pm 0.00	12.15 \pm 0.10
FedTAD	63.16 \pm 0.44	31.72 \pm 0.52	62.32 \pm 0.46	41.04 \pm 0.55	78.64 \pm 0.11	41.66 \pm 0.16	68.90 \pm 0.14	23.31 \pm 0.22	OOM	OOM
FedSpray	60.15 \pm 1.05	29.30 \pm 0.61	55.43 \pm 0.79	36.77 \pm 0.63	80.28 \pm 0.30	49.29 \pm 0.73	68.88 \pm 0.14	17.56 \pm 0.27	85.43 \pm 0.09	16.08 \pm 0.10
DENSE	63.24 \pm 0.32	31.74 \pm 0.44	61.71 \pm 0.21	40.69 \pm 0.44	78.59 \pm 0.15	41.63 \pm 0.31	68.81 \pm 0.04	22.97 \pm 0.18	86.95 \pm 0.01	21.14 \pm 0.00
Co-Boost	63.21 \pm 0.41	31.70 \pm 0.49	61.89 \pm 0.42	40.83 \pm 0.54	78.67 \pm 0.10	41.76 \pm 0.27	66.77 \pm 0.11	13.90 \pm 0.14	86.43 \pm 0.01	17.35 \pm 0.14
O-pFGL (Ours)	69.84 \pm 1.76	49.37 \pm 1.98	68.69 \pm 0.04	50.26 \pm 0.80	82.04 \pm 0.20	58.79 \pm 0.68	70.61 \pm 0.05	32.28 \pm 0.68	87.03 \pm 0.00	21.87 \pm 0.05

The state-of-the-art OFL methods (DENSE and Co-Boost) also have difficulty generating high-quality pseudo-data by the ensemble model when each model is trained on non-IID local graph data. FedTAD encounters OOM when handling million-scale graphs due to its graph diffusion operation, while our method remains scalable. FedGTA performs worst because its aggregation is based on the unreliable local models’ predictions under non-IID data in a single round. FedSpray focuses on minor classes, but it requires numerous communication for optimization, offering little advantage over others in one-shot communication.

Table 6: Performance of methods on datasets under Metis partition with 10 clients.

Method	Cora		CiteSeer		PubMed		ogbn-arxiv		ogbn-products	
	Acc.	F1								
Standalone	75.15 \pm 0.08	31.00 \pm 0.09	64.72 \pm 0.37	37.36 \pm 0.38	83.24 \pm 0.09	56.61 \pm 0.77	66.39 \pm 0.26	24.05 \pm 0.70	85.57 \pm 0.02	23.54 \pm 0.10
FedAvg	76.18 \pm 0.14	31.42 \pm 0.08	66.51 \pm 0.34	35.89 \pm 0.54	79.26 \pm 0.09	33.75 \pm 0.18	67.04 \pm 0.13	26.06 \pm 0.66	85.63 \pm 0.01	24.16 \pm 0.27
FedPUB	75.31 \pm 0.20	32.00 \pm 0.53	64.94 \pm 0.42	37.50 \pm 0.57	82.69 \pm 0.10	56.44 \pm 1.21	64.86 \pm 0.62	18.29 \pm 1.14	84.43 \pm 0.56	17.24 \pm 0.64
FedGTA	53.85 \pm 0.29	11.74 \pm 0.66	64.03 \pm 0.28	31.33 \pm 0.54	78.57 \pm 0.58	46.47 \pm 0.94	55.90 \pm 1.23	12.72 \pm 1.53	74.36 \pm 0.34	16.67 \pm 0.19
FedTAD	76.36 \pm 0.26	31.99 \pm 0.22	66.76 \pm 0.26	36.06 \pm 0.42	79.41 \pm 0.07	34.19 \pm 0.13	68.96 \pm 0.28	34.91 \pm 0.20	OOM	OOM
FedSpray	74.31 \pm 0.34	31.95 \pm 0.69	62.49 \pm 0.85	36.04 \pm 0.54	81.02 \pm 0.56	60.97 \pm 1.27	68.21 \pm 0.18	26.57 \pm 0.17	86.45 \pm 0.05	22.02 \pm 0.06
DENSE	76.21 \pm 0.08	31.64 \pm 0.24	65.62 \pm 0.27	37.88 \pm 0.24	79.29 \pm 0.05	33.81 \pm 0.09	68.89 \pm 0.04	34.34 \pm 0.34	86.43 \pm 0.03	28.42 \pm 0.25
Co-Boost	76.54 \pm 0.31	31.90 \pm 0.36	64.55 \pm 0.73	31.37 \pm 0.75	76.56 \pm 0.36	29.89 \pm 0.34	66.22 \pm 0.02	23.58 \pm 0.18	85.59 \pm 0.03	23.63 \pm 0.25
O-pFGL (Ours)	81.79 \pm 0.23	50.85 \pm 1.27	72.76 \pm 0.24	50.94 \pm 0.80	83.99 \pm 0.18	61.03 \pm 1.21	71.06 \pm 0.09	41.35 \pm 0.37	86.90 \pm 0.01	28.90 \pm 0.05

In addition to improving accuracy, our method consistently achieves a significant increase in F1-macro, an often overlooked metric in previous studies. This improvement highlights that our method enhances both personalization and generalization, resulting in more robust models.

We also compare our method with ReNode (Chen et al., 2021), a representative graph imbalance learning method, which targets to train robust graph models under imbalanced graph data. The comparison results are shown in Table 7. The results show that ReNode cannot effectively model the imbalanced graph data in our scenarios.

Table 7: Comparison with the graph imbalance learning method.

Louvain	Cora		CiteSeer		PubMed	
	Acc.	F1	Acc.	F1	Acc.	F1
ReNode	68.07 \pm 0.29	41.70 \pm 0.57	61.57 \pm 0.25	41.91 \pm 0.26	74.64 \pm 0.36	35.59 \pm 0.69
O-pFGL (Ours)	76.43 \pm 1.24	61.58 \pm 2.16	71.61 \pm 0.40	58.24 \pm 0.96	82.71 \pm 0.03	66.40 \pm 0.34
Metis	Cora		CiteSeer		PubMed	
	Acc.	F1	Acc.	F1	Acc.	F1
ReNode	76.44 \pm 0.06	27.69 \pm 0.45	65.89 \pm 0.23	37.74 \pm 0.15	78.81 \pm 0.14	32.94 \pm 0.18
O-pFGL (Ours)	81.79 \pm 0.23	50.85 \pm 1.27	72.76 \pm 0.24	50.94 \pm 0.80	83.99 \pm 0.18	61.03 \pm 1.21

Table 8: Performance of methods on datasets under Metis partition with 20 clients.

Method	Cora		CiteSeer		PubMed		ogbn-arxiv		ogbn-products	
	Acc.	F1								
Standalone	71.57 \pm 0.29	20.89 \pm 0.06	61.36 \pm 0.27	26.19 \pm 0.40	83.24 \pm 0.05	55.21 \pm 0.35	66.77 \pm 0.17	19.76 \pm 0.49	86.44 \pm 0.00	18.32 \pm 0.14
FedAvg	73.14 \pm 0.22	18.38 \pm 0.39	62.62 \pm 0.48	28.48 \pm 0.38	79.86 \pm 0.09	34.81 \pm 0.05	67.54 \pm 0.10	21.68 \pm 0.16	86.52 \pm 0.00	19.04 \pm 0.09
FedPUB	72.32 \pm 0.32	20.16 \pm 0.82	60.73 \pm 0.14	29.40 \pm 0.16	82.98 \pm 0.21	50.51 \pm 0.26	65.41 \pm 0.34	14.45 \pm 0.59	83.94 \pm 1.18	11.66 \pm 0.60
FedGTA	55.04 \pm 0.14	10.60 \pm 0.07	59.43 \pm 0.40	20.04 \pm 0.82	74.34 \pm 0.36	35.18 \pm 0.61	58.76 \pm 0.74	10.77 \pm 0.44	78.35 \pm 0.06	13.81 \pm 0.26
FedTAD	73.55 \pm 0.37	18.78 \pm 0.31	62.60 \pm 0.40	28.44 \pm 0.20	77.42 \pm 0.47	31.17 \pm 0.52	69.29 \pm 0.07	29.84 \pm 0.34	OOM	
FedSpray	71.44 \pm 0.04	21.49 \pm 0.15	58.98 \pm 1.87	29.35 \pm 1.52	81.05 \pm 0.33	40.51 \pm 0.56	68.86 \pm 0.44	22.49 \pm 0.44	85.28 \pm 0.05	17.31 \pm 0.04
DENSE	72.62 \pm 0.17	20.19 \pm 0.13	61.36 \pm 0.19	29.66 \pm 0.20	79.94 \pm 0.04	34.87 \pm 0.07	69.21 \pm 0.15	29.31 \pm 0.54	86.97 \pm 0.00	22.94 \pm 0.12
Co-Boost	73.42 \pm 0.06	18.45 \pm 0.24	61.30 \pm 0.56	25.87 \pm 0.78	79.98 \pm 0.06	35.04 \pm 0.27	66.72 \pm 0.06	19.48 \pm 0.28	86.43 \pm 0.01	18.51 \pm 0.24
O-pFGL (Ours)	78.31 \pm 0.88	37.21 \pm 1.96	68.88 \pm 0.22	41.95 \pm 0.25	83.94 \pm 0.05	56.61 \pm 1.36	70.87 \pm 0.18	36.06 \pm 0.43	87.15 \pm 0.02	23.41 \pm 0.26

Table 9: Comparison with FL methods with 100 communication rounds under Louvain partition.

Method	Cora		CiteSeer		PubMed		ogbn-arxiv		ogbn-products		Average	
	Acc.	F1	Acc.	F1								
FedAvg	75.27 \pm 0.17	61.74 \pm 0.21	67.11 \pm 0.48	51.86 \pm 0.81	85.22 \pm 0.14	71.17 \pm 0.22	68.10 \pm 0.07	30.72 \pm 0.14	86.58 \pm 0.02	28.28 \pm 0.07	76.46	48.75
FedPUB	78.32 \pm 0.37	64.59 \pm 0.80	69.00 \pm 0.74	56.43 \pm 0.68	83.12 \pm 0.08	70.18 \pm 0.36	65.34 \pm 0.28	12.50 \pm 0.20	85.18 \pm 0.14	16.31 \pm 0.46	76.19	44.00
FedGTA	73.32 \pm 0.17	60.08 \pm 0.32	67.12 \pm 1.58	52.68 \pm 1.81	84.39 \pm 0.08	72.06 \pm 0.12	58.30 \pm 0.30	12.22 \pm 0.26	83.25 \pm 0.17	24.71 \pm 0.10	73.28	44.35
FedTAD	74.62 \pm 0.44	60.37 \pm 1.01	67.68 \pm 0.39	53.43 \pm 0.82	84.70 \pm 0.21	68.56 \pm 0.72	68.77 \pm 0.12	27.33 \pm 0.50	OOM	OOM	N/A	N/A
FedSpray	70.08 \pm 0.41	56.46 \pm 1.30	68.31 \pm 0.88	55.07 \pm 0.94	84.04 \pm 0.10	74.06 \pm 0.29	70.20 \pm 0.08	34.09 \pm 0.33	84.06 \pm 0.11	20.80 \pm 0.05	75.34	48.10
O-pFGL (Ours)	76.43 \pm 1.24	61.58 \pm 2.16	71.61 \pm 0.40	58.24 \pm 0.96	82.71 \pm 0.03	66.40 \pm 0.34	70.93 \pm 0.59	36.66 \pm 0.22	86.63 \pm 0.02	27.21 \pm 0.15	77.66	50.02

A.2.2. COMPARED WITH MULTI-ROUNDS FL METHODS

To demonstrate the superiority of our method, we further compare our method with multi-round federated learning methods including FedAvg, FedPUB, FedGTA, FedTAD, and FedSpray. We set the communication round of the 5 methods to 100. The experimental results on 5 multi-scale graph datasets under Louvain and Metis partitions are shown in Table 9 and Table 10, respectively. Our method still outperforms in most cases and remains the best average performance.

A.2.3. FULL ABLATION STUDY

We conduct the ablation study to evaluate the performance gain of our method. We compare our method with 5 variants: (1) ft: we only fine-tune M_G to obtain M_i on local graph data, (2) ft_limb: we fine-tune with weighted cross entropy loss to handle data imbalance, (3) ft_dist: in the second stage fine-tuning, we perform distillation on all nodes by setting all γ_i to a fixed value in Eq. 17; (4) nd_ft_dist: we perform node adaptive distillation along with fine-tuning, without HRE, (5) ours: we perform the complete method (including HRE and personalized training with node-adaptive distillation), and (6) hre_nd_dist: we perform the complete method but without fine-tuning based on M_G from the first stage, instead training a model from scratch with cross-entropy loss and node-adaptive distillation.

Figure. 6 and Figure. 8 show our experimental results of accuracy and F1-macro under Louvain and Metis partition, respectively. We make the following 5 observations. **(O1)** Comparing ft and ft_focal, the focal loss in ft_limb cannot effectively address the non-IID graph data. We believe the reasons are that it’s hard to determine the proper weights under extreme non-IID scenarios. **(O2)** Comparing ft and ft_dist, a fixed distillation cannot balance the improvements of accuracy

Table 10: Comparison with FL methods with 100 communication rounds under Metis partition.

Method	Cora		CiteSeer		PubMed		ogbn-arxiv		ogbn-products		Average	
	Acc.	F1	Acc.	F1								
FedAvg	77.10 \pm 0.30	45.59 \pm 1.81	67.30 \pm 0.30	42.88 \pm 0.10	83.70 \pm 0.03	66.65 \pm 0.18	68.76 \pm 0.17	36.77 \pm 0.07	86.80 \pm 0.01	30.02 \pm 0.10	76.73	44.38
FedPUB	76.31 \pm 0.61	37.22 \pm 1.68	66.07 \pm 1.05	40.65 \pm 0.97	84.66 \pm 1.04	68.19 \pm 1.51	64.86 \pm 0.62	18.29 \pm 1.14	85.83 \pm 0.35	19.45 \pm 0.35	75.55	36.76
FedGTA	75.67 \pm 0.52	44.91 \pm 1.54	64.03 \pm 0.28	31.33 \pm 0.54	85.04 \pm 0.06	65.87 \pm 0.32	55.90 \pm 1.23	12.72 \pm 1.53	74.36 \pm 0.34	16.67 \pm 0.19	71.00	34.30
FedTAD	77.33 \pm 0.44	45.49 \pm 0.51	66.76 \pm 0.26	36.06 \pm 0.42	79.41 \pm 0.07	34.19 \pm 0.13	68.96 \pm 0.28	34.91 \pm 0.20	OOM		N/A	N/A
FedSpray	74.31 \pm 0.34	31.95 \pm 0.69	66.40 \pm 0.68	49.06 \pm 1.61	84.17 \pm 0.14	70.45 \pm 0.34	70.12 \pm 0.15	41.26 \pm 0.26	86.45 \pm 0.05	22.02 \pm 0.06	76.29	42.95
O-pFGL (Ours)	81.79 \pm 0.23	50.85 \pm 1.27	72.76 \pm 0.24	50.94 \pm 0.80	83.99 \pm 0.18	61.03 \pm 1.21	71.06 \pm 0.09	41.35 \pm 0.37	86.90 \pm 0.01	28.90 \pm 0.05	79.30	46.61

and F1-macro. We believe the reason is that it does not distinguish the majority and minority in the distillation. For nodes in major classes with high homophily, the global knowledge of M_G may have a negative impact, as demonstrated by the left panel in Figure 5. **(O3)** Comparing ft and nd_ft_dist, the node adaptive distillation is more flexible in determining when to introduce the global knowledge of M_G in fine-tuning. Thus nd_ft_dist achieves better accuracy and F1-macro. **(O4)** Comparing nd_ft_dist and ours, the HRE strategy further improves performance by generating a higher-quality global pseudo-graph through more precise estimations. **(O5)** Comparing ours and hre_nd_dist, we conclude that M_G provides better and necessary start-point for fine-tuning. Training the local personalized model from scratch, even with node-adaptive distillation and HRE, leads to a significant performance drop.

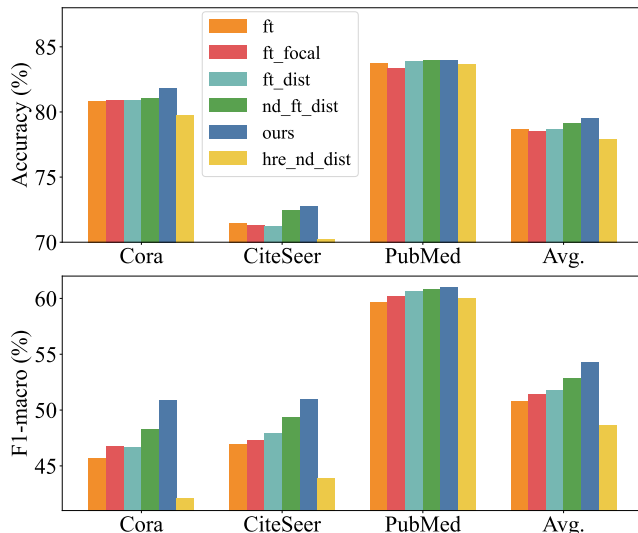


Figure 8: Ablation study under Metis partition.

We make a further ablation at the client level in Figure 5, evaluating different methods on a client using the CiteSeer dataset with the Louvain partition. As shown in the middle figure, class 3 and class 5 are regarded as major classes due to their larger quantity and relatively high homophily, while class 2 and class 1 are regarded as minor classes with fewer nodes and lower homophily. We make the following 3 observations. **(O1)** Compared to M_G , the ft method shows performance gain on major class 3 (+1.57%) and class 5 (+0.56%) but degrades performance on minor class 4 (-1.09%), class 2 (-2.78%), and class 1 (-3.22%). The performance differences after fine-tuning, shown in the left figure, align with the H values in the middle figure, highlighting the limitations of fine-tuning. **(O2)** The ft_dist method cannot handle this limitation effectively. With a fixed γ_i , the performance on major class 5 worsens (-0.42%), and the performance on minor classes still degrades. This phenomenon motivates us to develop node-adaptive distillation. **(O3)** Our method, with Class-aware Distillation Factor w_{dist} and node adaptive distillation, boosts performance on all classes by more than +2.4%.

We further justify the rationale for considering homophily in determining the major classes by H values in Eq. 2. The right panel of Figure 5 shows that while class 1 and class 4 have slightly more nodes, their average homophily is low (< 0.6), leading to less compact communities in the local graph. As a result, they are often neglected during fine-tuning, causing performance drops of -3.22% and -1.09%, respectively. In contrast, class 3 exhibits high average homophily (> 0.7), forming compact connections, allowing it to dominate the fine-tuning process with a performance improvement of +1.57%.

A.2.4. PERFORMANCE UNDER MODEL HETEROGENEITY

we conduct experiments on 10 clients with heterogeneous models. The model configuration is detailed in Section A.1. Under model heterogeneity, most pFGL methods (except FedTAD and FedSpray) do not work since they rely on the model parameter aggregation. Thus we compare our method with FedTAD, FedSpray, DENSE, and Co-Boost. The results under Louvain and Metis partitions are presented in Table 3 and Table 11. The results demonstrate the superior performance of our method in both accuracy and F1-macro.

Table 11: Performance of methods on 10 clients with heterogeneous models under Metis partition.

Metis	Cora		CiteSeer		ogbn-arxiv	
	Acc.	F1	Acc.	F1	Acc.	F1
Standalone	74.33 \pm 0.14	30.73 \pm 0.18	64.53 \pm 0.34	37.52 \pm 0.33	65.18 \pm 0.11	25.25 \pm 0.14
FedTAD	74.37 \pm 0.30	31.27 \pm 0.25	64.75 \pm 0.64	37.29 \pm 0.34	68.57 \pm 0.08	34.32 \pm 0.44
FedSpray	73.09 \pm 0.69	30.84 \pm 0.65	60.38 \pm 0.67	34.96 \pm 0.16	67.39 \pm 0.11	27.88 \pm 0.24
DENSE	73.51 \pm 0.99	30.62 \pm 0.42	65.33 \pm 0.24	37.62 \pm 0.09	68.56 \pm 0.03	34.64 \pm 0.03
Co-Boost	73.19 \pm 0.72	30.56 \pm 0.33	65.40 \pm 0.09	37.66 \pm 0.19	68.55 \pm 0.09	34.66 \pm 0.21
O-pFGL (Ours)	79.64 \pm 0.94	44.86 \pm 2.04	71.82 \pm 0.34	47.57 \pm 0.98	70.31 \pm 0.06	40.31 \pm 0.11

A.2.5. INDUCTIVE PERFORMANCE

We conduct experiments on three inductive graph datasets: Flickr, Reddit, and Reddit2, and vary the number of clients. Since Flickr has lower homophily, we use 2-layer SIGN (Frasca et al., 2020) for better graph learning. With 10 clients, experimental results under Louvain and Metis partitions are shown in Table 2 and Table 13, respectively. With 20 clients, experimental results under Louvain and Metis partitions are shown in Table 12 and Table 14, respectively. Our method is scalable and generally performs best.

Table 12: Performance on inductive datasets under Louvain partition with 20 clients.

Louvain	Flickr		Reddit		Reddit2	
	Acc.	F1	Acc.	F1	Acc.	F1
Standalone	42.10 \pm 0.14	15.39 \pm 0.25	89.90 \pm 0.06	13.08 \pm 0.21	91.09 \pm 0.02	16.52 \pm 0.04
FedAvg	28.86 \pm 1.96	13.55 \pm 0.36	83.99 \pm 0.28	7.81 \pm 0.08	85.94 \pm 0.30	8.48 \pm 0.06
FedPUB	42.06 \pm 0.00	8.31 \pm 0.00	90.34 \pm 0.08	11.95 \pm 0.27	91.23 \pm 0.02	13.96 \pm 0.11
FedGTA	40.78 \pm 4.26	14.11 \pm 1.51	89.83 \pm 0.05	12.90 \pm 0.32	91.14 \pm 0.05	16.64 \pm 0.12
FedTAD	41.61 \pm 0.42	15.88 \pm 0.31	OOM		OOM	
FedSpray	42.32 \pm 1.20	14.03 \pm 0.08	89.41 \pm 0.06	10.71 \pm 0.14	90.51 \pm 0.05	15.29 \pm 0.06
DENSE	42.45 \pm 0.72	11.67 \pm 1.07	89.89 \pm 0.05	14.27 \pm 0.14	91.25 \pm 0.03	18.14 \pm 0.44
Co-Boost	42.07 \pm 0.07	15.28 \pm 0.45	89.93 \pm 0.03	13.08 \pm 0.19	91.12 \pm 0.03	16.62 \pm 0.15
O-pFGL (Ours)	44.00 \pm 0.29	15.60 \pm 0.47	90.38 \pm 0.05	15.70 \pm 0.47	91.34 \pm 0.03	18.34 \pm 0.18

Table 13: Performance on inductive datasets under Metis partition with 10 clients.

Metis	Flickr		Reddit		Reddit2	
	Acc.	F1	Acc.	F1	Acc.	F1
Standalone	47.47 \pm 0.12	12.89 \pm 0.47	88.80 \pm 0.09	42.34 \pm 0.40	90.86 \pm 0.04	44.78 \pm 0.35
FedAvg	34.80 \pm 3.92	13.45 \pm 0.59	78.83 \pm 0.07	24.21 \pm 0.30	79.30 \pm 0.18	26.26 \pm 0.45
FedPUB	42.65 \pm 0.40	10.09 \pm 2.14	88.97 \pm 0.18	41.01 \pm 0.18	90.72 \pm 0.07	41.66 \pm 0.30
FedGTA	35.88 \pm 6.10	13.04 \pm 3.66	88.82 \pm 0.11	42.02 \pm 0.21	90.80 \pm 0.07	44.59 \pm 0.27
FedTAD	47.55 \pm 0.08	13.07 \pm 0.23	OOM		OOM	
FedSpray	43.77 \pm 1.58	13.37 \pm 0.42	87.71 \pm 0.18	41.65 \pm 0.29	89.99 \pm 0.23	43.74 \pm 0.26
DENSE	45.26 \pm 0.84	11.56 \pm 0.84	88.72 \pm 0.08	44.31 \pm 0.23	90.01 \pm 0.10	46.68 \pm 0.03
Co-Boost	47.42 \pm 0.10	12.90 \pm 0.61	88.71 \pm 0.07	42.08 \pm 0.27	90.81 \pm 0.06	44.56 \pm 0.20
O-pFGL (Ours)	47.89 \pm 0.11	13.11 \pm 0.34	89.59 \pm 0.10	45.31 \pm 0.36	91.16 \pm 0.04	48.56 \pm 0.31

A.2.6. MORE DATASETS

We further provide more experimental results on Computers, Photo, CS, and Physics datasets. Computers and Photo are Amazon co-purchase networks and CS and Physics are Co-author networks. The results under Louvain and Metis partitions are shown in Figure 15 and Figure 16, respectively. Our method consistently outperforms others in terms of both accuracy and F1-macro, which demonstrates the general advantages of our method.

A.2.7. DIFFERENT GNN ARCHITECTURES

To demonstrate the generality of our proposed method under different graph models, we conduct experiments with additional 3 prevalent graph models including 1) GraphSage (Hamilton et al., 2017), 2) GAT (Veličković et al., 2017), and 3) SGC (Wu

Table 14: Performance on inductive datasets under Metis partition with 20 clients.

Metis	Flickr		Reddit		Reddit2	
	Acc.	F1	Acc.	F1	Acc.	F1
Standalone	47.10 \pm 0.20	13.22 \pm 0.37	87.52 \pm 0.03	28.22 \pm 0.10	89.59 \pm 0.01	25.35 \pm 0.08
FedAvg	33.44 \pm 2.08	12.89 \pm 0.45	80.71 \pm 0.28	14.64 \pm 0.48	82.90 \pm 0.39	13.91 \pm 0.41
FedPUB	42.10 \pm 0.00	8.30 \pm 0.00	87.36 \pm 0.56	26.45 \pm 0.71	89.89 \pm 0.06	22.63 \pm 0.31
FedGTA	38.75 \pm 9.16	11.38 \pm 3.46	87.49 \pm 0.01	27.95 \pm 0.22	89.55 \pm 0.03	25.47 \pm 0.29
FedTAD	47.17 \pm 0.13	13.03 \pm 0.38	OOM		OOM	
FedSpray	43.35 \pm 0.96	14.00 \pm 0.55	86.66 \pm 0.09	27.60 \pm 0.20	88.99 \pm 0.01	24.23 \pm 0.39
DENSE	44.13 \pm 0.97	11.45 \pm 0.39	87.60 \pm 0.02	30.49 \pm 0.17	89.97 \pm 0.05	27.72 \pm 0.16
Co-Boost	47.08 \pm 0.22	13.11 \pm 0.66	87.52 \pm 0.06	28.09 \pm 0.12	89.67 \pm 0.07	25.62 \pm 0.22
O-pFGL (Ours)	47.08 \pm 0.27	13.37 \pm 0.24	88.28 \pm 0.01	31.01 \pm 0.47	90.25 \pm 0.07	30.74 \pm 0.25

Table 15: Performance of methods on more datasets under the Louvain partition.

Method	Computers		Photo		CS		Physics	
	Acc.	F1	Acc.	F1	Acc.	F1	Acc.	F1
Standalone	87.34 \pm 0.06	38.27 \pm 0.91	89.16 \pm 0.20	40.46 \pm 1.31	87.18 \pm 0.02	42.97 \pm 0.07	93.65 \pm 0.06	68.40 \pm 0.53
FedAvg	87.18 \pm 0.75	38.94 \pm 0.51	89.26 \pm 0.13	41.11 \pm 0.77	87.10 \pm 0.11	44.86 \pm 0.23	93.55 \pm 0.03	70.72 \pm 0.38
FedPUB	83.51 \pm 2.46	31.48 \pm 2.64	89.43 \pm 0.05	38.17 \pm 1.24	87.01 \pm 0.12	41.99 \pm 0.38	93.55 \pm 1.22	64.95 \pm 1.91
FedGTA	56.73 \pm 14.13	13.41 \pm 3.08	53.68 \pm 3.75	15.09 \pm 1.37	83.26 \pm 0.11	40.34 \pm 1.10	91.81 \pm 0.22	64.34 \pm 0.77
FedTAD	87.08 \pm 0.59	38.71 \pm 1.00	89.61 \pm 0.27	41.91 \pm 1.14	87.15 \pm 0.06	44.80 \pm 0.05	93.51 \pm 0.04	70.52 \pm 0.53
FedSpray	86.67 \pm 2.31	28.56 \pm 4.74	87.40 \pm 0.50	35.59 \pm 0.92	86.58 \pm 0.35	38.69 \pm 1.36	92.01 \pm 0.90	48.68 \pm 1.13
DENSE	87.19 \pm 0.44	39.18 \pm 0.36	89.36 \pm 0.22	41.87 \pm 0.55	87.15 \pm 0.07	44.92 \pm 0.25	93.52 \pm 0.04	70.02 \pm 0.42
Co-Boost	87.56 \pm 0.53	38.98 \pm 0.82	89.52 \pm 0.24	41.54 \pm 0.65	87.18 \pm 0.12	44.87 \pm 0.30	93.54 \pm 0.03	70.45 \pm 0.36
O-pFGL (Ours)	88.30 \pm 0.06	44.01 \pm 1.93	90.24 \pm 0.09	48.25 \pm 1.79	90.00 \pm 0.12	53.88 \pm 1.15	94.21 \pm 0.22	71.17 \pm 1.35

Table 16: Performance of methods on more datasets under the Metis partition.

Metis+	Computers		Photo		CS		Physics	
	Acc.	F1	Acc.	F1	Acc.	F1	Acc.	F1
Standalone	87.50 \pm 0.34	25.43 \pm 0.69	90.62 \pm 1.41	29.70 \pm 0.16	87.39 \pm 0.13	42.30 \pm 0.35	93.89 \pm 0.04	65.11 \pm 0.20
FedAvg	87.36 \pm 0.30	24.85 \pm 1.69	90.76 \pm 0.45	30.33 \pm 1.13	87.14 \pm 0.03	42.10 \pm 0.05	93.65 \pm 0.08	64.16 \pm 0.50
FedPUB	85.20 \pm 1.11	19.76 \pm 1.52	89.66 \pm 0.30	23.64 \pm 1.85	87.30 \pm 0.14	42.00 \pm 0.47	93.99 \pm 0.06	62.92 \pm 0.96
FedGTA	74.36 \pm 4.49	15.48 \pm 1.66	53.68 \pm 3.76	15.09 \pm 1.37	87.49 \pm 0.03	42.59 \pm 0.11	84.00 \pm 3.98	23.27 \pm 0.77
FedTAD	87.64 \pm 0.32	24.43 \pm 0.31	90.66 \pm 0.36	29.64 \pm 1.44	87.15 \pm 0.02	42.15 \pm 0.21	93.58 \pm 0.03	63.77 \pm 0.17
FedSpray	86.34 \pm 0.49	21.72 \pm 1.82	88.77 \pm 0.49	21.34 \pm 0.98	81.50 \pm 0.29	38.04 \pm 0.26	91.17 \pm 0.12	60.79 \pm 0.78
DENSE	87.75 \pm 0.29	23.99 \pm 0.65	91.14 \pm 0.21	31.40 \pm 1.16	87.12 \pm 0.08	42.04 \pm 0.33	93.59 \pm 0.07	64.03 \pm 0.44
Co-Boost	87.32 \pm 0.80	22.66 \pm 1.74	90.97 \pm 0.18	30.77 \pm 0.73	87.12 \pm 0.03	42.04 \pm 0.08	93.57 \pm 0.08	63.69 \pm 0.68
O-pFGL (Ours)	88.59 \pm 0.13	33.01 \pm 3.66	91.79 \pm 0.13	42.39 \pm 0.81	89.96 \pm 0.20	50.33 \pm 1.01	94.51 \pm 0.09	66.41 \pm 1.24

et al., 2019). The experimental results under Louvain and Metis partitions are shown in Table 17 and Table 18, respectively. Our method show consistent advantages over other methods.

Table 17: Performance of methods with different GNN architectures under Louvain partition.

Method	GraphSage						GAT						SGC					
	Cora		CiteSeer		ogbn-arxiv		Cora		CiteSeer		ogbn-arxiv		Cora		CiteSeer		ogbn-arxiv	
	Acc.	F1																
Standalone	66.35	38.60	59.50	39.87	67.30	20.33	68.79	43.37	60.42	40.49	67.76	20.41	65.53	39.71	60.28	41.15	59.17	9.19
FedAvg	66.63	40.82	57.59	38.86	50.05	3.10	69.82	45.56	62.83	45.27	51.51	3.55	66.44	39.02	63.00	42.32	59.49	9.45
FedPUB	43.27	18.83	44.15	28.93	41.12	7.91	66.35	42.52	66.75	49.93	56.69	12.14	57.21	42.04	65.60	49.63	35.36	9.31
FedGTA	47.25	26.43	65.55	49.46	58.59	14.48	47.89	30.40	65.96	51.17	59.70	15.48	48.40	32.90	64.26	46.59	53.25	8.32
FedTAD	66.82	40.87	57.14	38.31	68.78	29.83	69.63	45.58	60.22	43.63	50.04	3.55	69.59	43.68	64.36	46.04	65.38	17.76
FedSpray	63.75	37.49	54.08	37.84	47.85	2.26	62.91	39.32	61.05	44.21	47.52	2.16	63.40	35.54	60.63	41.19	65.38	17.76
DENSE	66.78	40.46	57.96	39.13	50.29	3.18	70.40	47.25	58.99	42.31	69.33	28.78	69.74	43.87	64.04	45.67	62.72	14.88
Co-Boost	65.34	39.98	54.80	35.54	68.74	29.98	70.37	47.34	59.28	42.40	69.32	28.93	68.81	44.39	64.02	45.68	62.72	14.89
O-pFGL (Ours)	72.80	54.92	69.05	54.86	69.07	32.81	75.03	57.77	71.23	57.36	70.41	34.86	73.65	54.70	69.47	54.04	70.31	35.66

Table 18: Performance of methods with different GNN architectures under Metis partition.

Method	GraphSage						GAT						SGC					
	Cora		CiteSeer		ogbn-arxiv		Cora		CiteSeer		ogbn-arxiv		Cora		CiteSeer		ogbn-arxiv	
	Acc.	F1																
Standalone	74.78	24.62	64.22	35.94	67.42	28.75	75.96	29.95	64.42	37.70	67.26	27.12	76.11	30.38	63.97	36.34	58.49	12.63
FedAvg	74.89	26.16	65.14	36.46	50.04	4.10	75.01	29.16	65.66	37.58	49.51	3.83	75.48	23.69	66.78	36.34	58.99	13.16
FedPUB	49.67	16.75	50.44	30.02	43.30	9.55	72.97	28.86	65.67	38.10	58.92	16.23	51.50	27.93	60.36	40.17	35.62	8.88
FedGTA	53.42	13.48	64.86	31.57	55.65	12.00	53.67	13.76	65.90	34.49	54.81	12.88	54.67	16.28	64.67	29.34	54.11	10.27
FedTAD	74.98	26.80	63.63	35.32	68.56	35.21	75.17	30.61	63.06	36.35	50.04	3.55	76.47	31.17	65.40	37.54	63.74	22.61
FedSpray	72.79	23.95	59.21	33.27	47.45	2.69	74.84	30.56	63.97	36.79	45.46	2.18	75.86	25.96	65.74	36.17	65.40	24.64
DENSE	74.71	26.24	64.41	36.13	50.19	4.18	75.48	31.11	63.08	35.96	69.08	35.09	76.39	31.14	65.40	37.61	63.74	22.52
Co-Boost	74.56	26.69	62.27	33.17	68.53	35.08	75.44	31.09	63.32	36.27	69.14	35.09	76.42	31.15	65.42	37.62	63.74	22.52
O-pFGL (Ours)	78.48	44.59	69.55	48.17	69.20	36.57	80.68	50.02	71.91	49.03	69.98	37.83	79.96	44.48	71.58	46.87	70.26	40.10

A.3. Complexity Analysis

We provide complexity analysis of methods from three perspectives: communication, computation, and memory, with a 2-layer GCN model as an example.

Table 19: Communication complexity of methods.

Communication	Upload	Download
Standalone	N/A	N/A
FedAvg	$O(fd + dC)$	$O(fd + dC)$
FedPUB	$O(fd + dC)$	$O(fd + dC)$
FedGTA	$O(fd + dC + kKc)$	$O(fd + dC)$
FedTAD	$O(fd + dC)$	$O(fd + dC)$
FedSpray	$O(fd' + d'C)$	$O(fd' + d'C)$
DENSE	$O(fd + dC)$	$O(fd + dC)$
Co-Boost	$O(fd + dC)$	$O(fd + dC)$
O-pFGL (Ours)	$O(Chf)$	$O(n'f + n'^2)$

Communication Analysis We provide communication analysis of methods in Table 19. FedAvg, FedPUB, FedTAD, DENSE, and Co-Boost all need to upload and download the whole model parameters ($O(fd + dc)$, where d is the hidden dimension). FedGTA need to upload additional mixed moments of neighboring features ($O(kKc)$, where K is the order of the moment and k is the propagation steps of Label Propagation) for personalized aggregation. FedSpray needs to upload and download the global feature-structure encoder and structure proxy ($O(fd' + d'c)$, where d' is the output dimension of

the encoder and dimension of the structure proxy). Our method only needs to upload the class-wise statistics ($O(chf)$) and download the generated global pseudo-graph ($O(n'f + n'^2)$, n' is the number of nodes in the global pseudo-graph, which is usually a small value as indicated in Section A.1). The communication costs of our method are independent of the model size. The larger the model gets, the more communication-efficient our method is compared with other methods.

Table 20: Computation complexity of methods.

Computation	Client	Server
Standalone	$O(m(f + d) + nd(f + C))$	N/A
FedAvg	$O(m(f + d) + nd(f + C))$	$O(N(fd + dC))$
FedPUB	$O(m(f + d) + nd(f + C))$	$O(N^2(fd + dC) + Kn'^2)$
FedGTA	$O(m(f + d + kC) + nd(f + C))$	$O(N^2(fd + dC + kKc))$
FedTAD	$O(pn^2 + m(f + d) + nd(f + C))$	$O(N(fd + dC) + n'^2f + N(m'(f + d) + n'(d(f + C)))) + L'n'd'^2$
FedSpray	$O(m(f + d) + nd(f + C) + nfd' + nd'C)$	$O(Nfd')$
DENSE	$O(m(f + d) + nd(f + C))$	$O(N(fd + dC) + n'^2f + N(m'(f + d) + n'(d(f + C)))) + L'n'd'^2$
Co-Boost	$O(m(f + d) + nd(f + C))$	$O(N(fd + dC) + n'^2f + N(m'(f + d) + n'(d(f + C)))) + L'n'd'^2$
O-pFGL (Ours)	$O(m(f + d) + nd(f + C))$	$O(NChf + m'f + Chf + n'^2f)$

Computation Analysis We provide computation analysis of methods in Table 20. we slightly abuse the notation by redefining the number of clients as N , the number of edges in local graph data as m , and the number of nodes in local graph data as n . K' is the number of proxy graphs generated in FedPUB and n' is the number of nodes in each proxy graph. p is the diffusion step in FedTAD and $O(pn^2)$ is the complexity to calculate the topology embedding, which could be highly computation-expensive. For FedTAD, DENSE, and Co-Boost, $O(n'^2f)$ is the complexity of constructing the generated graph. L' is the number of layers of the generator, f' is the dimension of the latent features in the generator and n' is the number of generated nodes. $O(L'n'd'^2)$ is the complexity of forwarding of the generator in the server. For our method, $O(NChf)$ is the complexity of aggregating the statistics. m' is the estimated number of edges in the generated global pseudo-graph, usually a small value. $O(m'f + Chf)$ is the complexity of calculating alignment loss. $O(n'^2f)$ is the complexity of calculating the smoothness loss. The computation complexity on clients in our method is kept as least as possible, the same as the vanilla FedAvg and Standalone.

Table 21: Memory complexity of methods.

Memory	Client	Server
Standalone	$O(fd + dC)$	N/A
FedAvg	$O(fd + dC)$	$O(N(fd + dC))$
FedPUB	$O(fd + dC)$	$O(N(fd + dC) + K'n'f)$
FedGTA	$O(fd + dC + kKc)$	$O(N(fd + dC + kKc))$
FedTAD	$O(fd + dC + pn^2)$	$O(N(fd + dC) + n'f + n'^2)$
FedSpray	$O(fd + dC + fd' + d'C + nd')$	$O(Nnd' + f'd' + d'C)$
DENSE	$O(fd + dC)$	$O(N(fd + dC) + n'f + n'^2)$
Co-Boost	$O(fd + dC)$	$O(N(fd + dC) + n'f + n'^2)$
O-pFGL (Ours)	$O(fd + dC)$	$O(Nchf + n'f + n'^2)$

Memory Analysis We provide memory analysis of methods in Table 21. Standalone, FedAvg, FedPUB, DENSE, and Co-Boost only need to store the model parameters ($O(fd + dC)$). FedTAD needs to additionally store the topology embedding calculated by graph diffusion ($O(pn^2)$), thus it faces OOM on larger graphs. FedSpray needs to store additional encoders and structure proxy. For FedTAD, DENSE, Co-Boost, and our method, the server needs to additionally store the generated graph, which costs approximately $O(n'f + n'^2)$ memory. Since n' is usually a small value, it would incur much memory overhead on the server.

A.4. An Equivalent Server-Efficient Variant Method

An equivalent variant of our method is to move the global pseudo-graph generation process to the clients. Specifically, the server only securely aggregates the uploaded statistics and then distributes $\{N^c, \mu^c, s^{2^c}\}$ to clients (with Homomorphic Encryption (Acar et al., 2018)). Then the clients generate the global pseudo-graph with aggregated statistics locally. It still supports model heterogeneity and Secure Aggregation protocols. This variant enables extreme efficiency on the server since the server only needs to perform a series of weighted average operations, moving the computation overhead of global pseudo-graph generation to the client-side.

A.5. Experimental Results on a Large Number of Clients

We conduct experiments on a large number of clients to evaluate the robustness of our method. We simulate 10, 100, and 1000 clients on ogbn-products with Metis partition. The F1-macro metrics of methods are shown in Figure 9. Our method consistently outperforms other methods on a large number of clients.

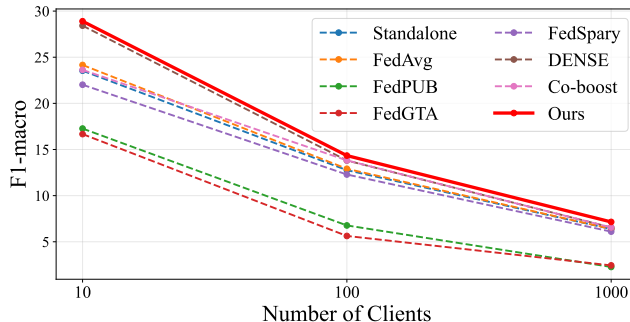


Figure 9: Performance of method with a large number of clients on ogbn-products dataset under Metis partition.

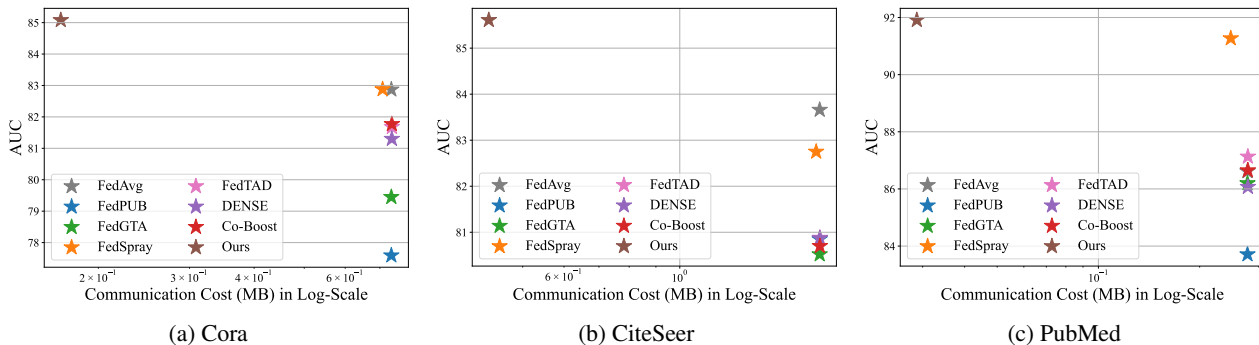


Figure 10: Performance of method on the subsequent link prediction task on Cora, CiteSeer, PubMed datasets. The x-axis is set to the logarithmic scale.

A.6. Experimental Results on Link Prediction Task

To evaluate the effectiveness of the methods of node representation learning, we perform the link prediction task. We first perform the node classification task to pre-train a GCN as the feature encoder with a classification head to generate distinguishable node representation and then fine-tune the feature encoder for link prediction. The experimental results (take AUC as our metrics) are shown in Figure 10, which shows that our method learns better node representation and achieves the best on the subsequent link prediction task while having less communication cost.